

# The Membrane Protein of Severe Acute Respiratory Syndrome Coronavirus Functions as a Novel Cytosolic Pathogen-Associated Molecular Pattern To Promote Beta Interferon Induction via a Toll-Like-Receptor-Related TRAF3-Independent Mechanism

Yi Wang, Li Liu

Department of Microbiology, Institute of Basic Medical Sciences, Chinese Academy of Medical Sciences and School of Basic Medicine, Peking Union Medical College, Beijing, China

**ABSTRACT** Most of the intracellular pattern recognition receptors (PRRs) reside in either the endolysosome or the cytoplasm to sense pathogen-derived RNAs, DNAs, or synthetic analogs of double-stranded RNA (dsRNA), such as poly(I:C). However, it remains elusive whether or not a pathogen-derived protein can function as a cytosolic pathogen-associated molecular pattern (PAMP). In this study, we demonstrate that delivering the membrane gene of severe acute respiratory syndrome coronavirus (SARS-CoV) into HEK293T, HEK293ET, and immobilized murine bone marrow-derived macrophage (J2-M $\phi$ ) cells significantly upregulates beta interferon (IFN- $\beta$ ) production. Both NF- $\kappa$ B and TBK1-IRF3 signaling cascades are activated by M gene products. M protein rather than M mRNA is responsible for M-mediated IFN- $\beta$  induction that is preferentially associated with the activation of the Toll-like receptor (TLR) adaptor proteins MyD88, TIRAP, and TICAM2 but not the RIG-I signaling cascade. Blocking the secretion of M protein by brefeldin A (BFA) failed to reverse the M-mediated IFN- $\beta$  induction. The antagonist of both TLR2 and TLR4 did not impede M-mediated IFN- $\beta$  induction, indicating that the driving force for the activation of IFN- $\beta$  production was generated from inside the cells. Inhibition of TRAF3 expression by specific small interfering RNA (siRNA) did not prevent M-mediated IFN- $\beta$  induction. SARS-CoV pseudovirus could induce IFN- $\beta$  production in an M rather than M(V68A) dependent manner, since the valine-to-alanine alteration at residue 68 in M protein markedly inhibited IFN- $\beta$  production. Overall, our study indicates for the first time that a pathogen-derived protein is able to function as a cytosolic PAMP to stimulate type I interferon production by activating a noncanonical TLR signaling cascade in a TRAF3-independent manner.

**IMPORTANCE** Viral protein can serve as a pathogen-associated molecular pattern (PAMP) that is usually recognized by certain pathogen recognition receptors (PRRs) on the cell surface, such as Toll-like receptor 2 (TLR2) and TLR4. In this study, we demonstrate that the membrane (M) protein of SARS-CoV can directly promote the activation of both beta interferon (IFN- $\beta$ ) and NF- $\kappa$ B through a TLR-related signaling pathway independent of TRAF3. The driving force for M-mediated IFN- $\beta$  production is most likely generated from inside the cells. M-mediated IFN- $\beta$  induction was confirmed at the viral infection level since a point mutation at the V68 residue of M markedly inhibited SARS-CoV pseudovirally induced IFN- $\beta$  production. Thus, the results indicate for the first time that SARS-CoV M protein may function as a cytosolic PAMP to stimulate IFN- $\beta$  production by activating a TLR-related TRAF3-independent signaling cascade.

Received 29 October 2015 Accepted 8 January 2016 Published 9 February 2016

**Citation** Wang Y, Liu L. 2016. The membrane protein of severe acute respiratory syndrome coronavirus functions as a novel cytosolic pathogen-associated molecular pattern to promote beta interferon induction via a Toll-like-receptor-related TRAF3-independent mechanism. *mBio* 7(1):e01872-15. doi:10.1128/mBio.01872-15.

**Editor** Xiang-Jin Meng, Virginia Polytechnic Institute and State University

**Copyright** © 2016 Wang and Liu. This is an open-access article distributed under the terms of the [Creative Commons Attribution-Noncommercial-ShareAlike 3.0 Unported license](https://creativecommons.org/licenses/by-nc-sa/4.0/), which permits unrestricted noncommercial use, distribution, and reproduction in any medium, provided the original author and source are credited.

Address correspondence to Li Liu, [lliu@pumc.edu.cn](mailto:lliu@pumc.edu.cn).

The innate immune response is the first line of the host immune response against invading pathogens such as viruses (1–3). After entry into the cell, the virus releases its genetic contents, such as DNAs or RNAs, into the cytosol. The host cells possess a number of pattern recognition receptors (PRRs) that are able to detect viral infection by acting as viral nucleic acid sensors. Three major classes of PRRs have been identified and intensively studied. They include Toll-like receptors (TLRs), retinoic acid-inducible gene 1 (RIG-I)-like receptors (RLRs), and NOD-like receptors (NLRs) (2).

TLRs interact with their ligands through the recognition of certain pathogen-associated molecular patterns (PAMP). MyD88

and TRIF are two important adaptor proteins in TLR-mediated type I interferon (IFN-I) production (4). TLR could induce the production of type I interferon by MyD88-dependent or MyD88-independent mechanisms. Differently from TLR3/TLR4, which use TRIF as an adaptor, the other TLRs induce beta interferon (IFN- $\beta$ ) production through the adaptor MyD88. TLR3 can bind viral double-stranded RNA (dsRNA) to induce type I interferon production, while TLR4 mainly binds to lipopolysaccharide (LPS) to stimulate the IFN- $\beta$  response. Differently, TLR7 and TLR9 could recognize single-stranded RNA (ssRNA) and CpG DNA, respectively, to induce IFN- $\beta$  production (5, 6).

In addition to the TLR, which can be defined as a membrane-associated PRR, another set of PRRs is localized at the cytoplasm and mainly includes RIG-like receptors (RLRs) and NOD-like receptors (NLRs) to sense viral dsRNAs and bacterial cell wall components, respectively (2, 7). The RLRs consist of at least three members, including RIG-I, MDA5, and LGP2. RIG-I recognizes 5'-triphosphate RNA and short dsRNA (4, 8), while MDA5 senses long dsRNA (9). An adaptor protein, MAVS, is required for the activation of the RIG-I/MDA5 signaling pathway. The association of viral nucleic acids with MAVS promotes the aggregation of MAVS on the mitochondrial membrane (10). The "ligation" of TRAF3 with the aggregated MAVS may promote the phosphorylation of IRF3 that is required for IFN- $\beta$  production (11). A recent study also shows that an endoplasmic reticulum (ER)-derived adaptor protein, STING, could also function downstream of MAVS to promote IRF3 phosphorylation and the subsequent IFN- $\beta$  response (12).

Pathogen-derived proteins such as virus-encoded proteins are frequently documented as negative regulators in subverting type I interferon (IFN-I) induction by interfering with a certain key component(s) of IFN-I activation signaling cascades. Viral evolution may develop a unique strategy to inhibit host innate immunity by generating virus-derived antagonists to some key signaling molecules. The vaccinia virus encodes two Toll/interleukin-1 (IL-1) receptor (TIR) domains containing proteins A46R and A52R, which can negatively regulate TLR signaling by two distinct mechanisms (13). The vaccinia virus A46R inhibits TLR signaling by physically interacting with the BB loop of TIR containing adaptor proteins such as MyD88 adaptor-like (MAL) and TRIF-related adaptor molecule (TRAM) to disrupt receptor-adaptor (e.g., TLR4-MAL and TLR4-TRAM) interactions (14, 15). Differently, the A52R protein may function as a dominant negative MyD88 to directly interact with TRAF6 and IRAK2 (16, 17). On the other hand, the vaccinia virus N1L protein, another protein homologous to A52R, employs a different anti-IFN-I strategy by targeting both the TBK1/IKK kinase (IKK $\epsilon$ ) and IKK $\alpha$ /IKK $\beta$  complexes to inhibit IRF3 and NF- $\kappa$ B signaling, respectively (18). Alternatively, virus may invade the cells to target the retinoic acid-inducible gene I (RIG-I)-like receptor signaling pathways for the prevention of IFN-I induction. For example, the influenza virus nonstructural protein NS1 can sequester either the dsRNA or 5'-triphosphate RNA products of viral infection which can be sensed by or directly bound to the RNA helicase sensor RIG-I to inhibit RIG-I-mediated IFN- $\beta$  production (8, 19, 20). The paramyxovirus V protein inhibits IFN- $\beta$  induction through the blockage of MDA5, another RIG-I-homologous cytosolic dsRNA sensor (21). A recent study revealed that the transcriptional factor IRF3 might be alternatively targeted and inhibited by the paramyxovirus V protein to impede IFN- $\beta$  gene transcription (22).

It has been demonstrated in some cases that viral proteins may function as extracellular PAMPs to activate the IFN-I immune response, most often through TLR (such as TLR2 and TLR4) signaling pathways (23–25). However, evidence is lacking in regard to whether or not a virus-derived protein can function as a cytosolic PAMP.

Our initial study indicates that delivering the membrane gene into HEK293 cells markedly induces type I interferon (IFN-I) production (26). To our knowledge, there are limited reports regarding the induction of IFN- $\beta$  expression directly by viral structural genes. Therefore, it is intriguing to know which mechanism is responsible for the severe acute respiratory syndrome coronavirus

(SARS-CoV) M gene-mediated IFN- $\beta$  response. In this study, we demonstrate that SARS-CoV M protein, rather than its mRNA, activates IFN- $\beta$  and NF- $\kappa$ B responses through TLR-related TRAF3-independent signaling cascades. The driving force for M-mediated IFN- $\beta$  induction was most likely generated from the inside of the cells. Using SARS-CoV pseudovirus as an infectious agent, we further show that single point mutation at the valine 68 residue of M protein markedly inhibits virus-induced IFN- $\beta$  production. Overall, SARS-CoV M protein may stand out as a novel cytosolic PAMP in mediating the IFN- $\beta$  immune response.

## RESULTS

**The SARS-CoV M gene stimulates beta interferon gene expression in the human embryonic kidney 293T cell line.** The overexpression of the SARS-CoV M gene has been shown to upregulate the transcriptional level of IFN- $\beta$  (26). To further confirm the result, using either enhanced green fluorescent protein (EGFP) or poly(I:C) as a negative or positive control, respectively, we demonstrated that M gene products specifically promoted IFN- $\beta$  production, since cotransfection with M small interfering RNA (siRNA) completely abolished M-mediated IFN- $\beta$  induction at both protein (Fig. 1A, comparing lanes 3 and 4) and mRNA (Fig. 1B) levels. Moreover, after a 48-h transfection, cell supernatants were collected and assayed for the presence of IFN- $\beta$  by enzyme-linked immunosorbent assay (ELISA). Figure 1C clearly demonstrated that delivering pCMV-Myc-M into HEK293T cells specifically and significantly promoted the secretion of IFN- $\beta$  into cell culture medium. In addition, the promoter sequence of IFN- $\beta$  was placed upstream of the firefly luciferase reporter to generate the pGL3-IFN- $\beta$ -Luc construct. To test the specificity of M-mediated IFN- $\beta$  induction, other viral envelope-associated genes such as the spike (S) and envelope (E) protein genes as well as the M mutant [M(V68A)] from the GZ50 isolate were also included (27). The result of a dual-luciferase assay using the *Renilla* luciferase gene as a transfection control demonstrated that the SARS-CoV M gene rather than the S and E genes markedly increased IFN- $\beta$  promoter activity (Fig. 1D), whereas the valine-to-alanine alteration at residue 68 of M protein completely abolished this induction, indicating that the specificity of M gene products played a role in this process. Consistent with these results, Western blotting and ELISA further validated the above observation (Fig. 1E and F). To detect if the SARS-CoV M gene has a direct effect on NF- $\kappa$ B activation, pCMV-Myc-M was cotransfected with pNF $\kappa$ B-luc, which contained five copies of NF- $\kappa$ B recognition sites, into HEK293T cells. The results of the dual-luciferase assay revealed that the SARS-CoV M gene specifically and dramatically upregulated NF- $\kappa$ B activity compared with the controls (Fig. 1G). Moreover, M could mediate IFN- $\beta$  induction in both dose- and time-dependent manner (Fig. 1H and I). Overall, the data strongly indicated that the SARS-CoV M gene product was sufficient to promote IFN- $\beta$  gene expression.

**The SARS-CoV M gene product activates the IFN- $\beta$  signaling pathway at or upstream of TBK1.** To further confirm the above results, increased doses of the pCMV-Myc-M gene were transiently transfected into HEK293ET cells. The cell lysates prepared from the transfection were examined for the activation of the downstream modulator and/or effector molecules, such as TBK1, IRF3, and NF- $\kappa$ B. Figure 2A clearly demonstrates that SARS-CoV M gene products not only enhanced the phosphorylation level of TBK1 but also promoted the activation of both NF- $\kappa$ B p65 and

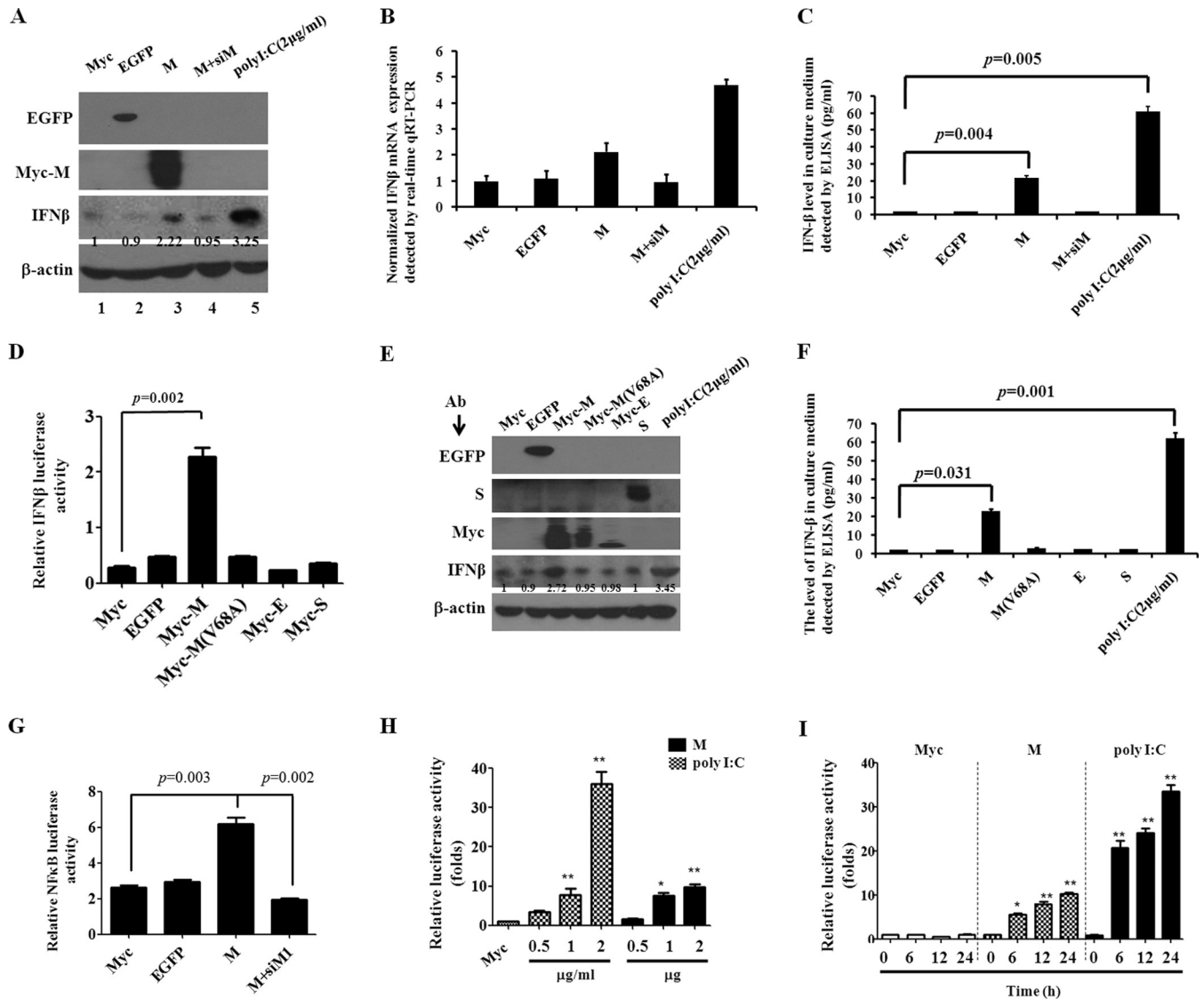


**FIG 1** SARS-CoV M gene product significantly upregulates both IFN- $\beta$  and NF- $\kappa$ B gene expression in HEK293T cells. (A) SARS-CoV M gene products upregulate IFN- $\beta$  protein expression. HEK293T cells were individually transfected with pCMV-Myc, pEGFP, pCMV-Myc-M, pCMV-Myc-M plus pBS-U6-siM1, and poly(I:C). After 48 h of transfection, the reaction products were subjected to Western blot analysis. The expression of  $\beta$ -actin served as a loading control. The relative band intensity was quantitated by the Image J program in comparison with the  $\beta$ -actin control. The result is representative of two identical experiments. (B) Real-time qRT-PCR analysis on M-mediated IFN- $\beta$  expression. HEK293T cells were individually transfected with pCMV-Myc, pEGFP, pCMV-Myc-M, pCMV-Myc-M plus pBS-U6-siM1, and poly(I:C). After 48 h of transfection, total RNAs were isolated from each transfection. Real-time qRT-PCR was employed for the detection of IFN- $\beta$  RNA expression. The result is representative of at least 2 identical experiments. The IFN- $\beta$  mRNA level was normalized by using  $\beta$ -actin mRNA as an internal control. (C) ELISA of M-mediated IFN- $\beta$  expression. The transfection was performed in the same way as that in panel B. After 48 h of transfection, the cell supernatants were harvested and subjected to ELISA. Each value represents the mean  $\pm$  standard deviation from three independent tests. (D) Dual-luciferase assay on the specificity of M-mediated IFN- $\beta$  induction. Plasmid DNAs [pCMV-Myc, pEGFP, pCMV-Myc-M, pCMV-Myc-M(V68A), pCMV-Myc-E, and pCMV-Myc-S] were individually cotransfected with pGL3-IFN- $\beta$ -luciferase reporter (100 ng) plus pRL-TK (10 ng) into HEK293T cells. After 48 h of transfection, the dual-luciferase assay was performed to detect the M-mediated IFN- $\beta$  expression. Each value represents the mean  $\pm$  standard deviation from three independent tests. (E) Western blotting on the specificity of M-mediated IFN- $\beta$  induction. Plasmid DNAs [pCMV-Myc, pEGFP, pCMV-Myc-M, pCMV-Myc-M(V68A), pCMV-Myc-E, pCMV-Myc-S, and poly(I:C)] were transiently transfected into HEK293T cells. After 48 h of transfection, whole-cell lysates were harvested and subjected to Western blotting by using specific antibodies (Ab) as indicated. The expression of  $\beta$ -actin served as a loading control. The relative band intensity was quantitated with the Image J program in comparison with the  $\beta$ -actin control. The result is representative of at least 3 identical experiments. (F) ELISA of M-mediated IFN- $\beta$  secretion in cell culture medium. The transfection was performed in the same way as that in panel E. After 48 h of transfection, the cell supernatants were harvested and subjected to ELISA. Each value represents the mean  $\pm$  standard deviation from three independent tests. (G) The SARS-CoV M gene stimulates NF- $\kappa$ B activation. About 100 ng of pGL3-NF- $\kappa$ B was cotransfected with 2  $\mu$ g of either Myc vector, EGFP, pCMV-Myc-M, or pCMV-Myc-M plus pBS-U6-siM1. Each transfection mixture also contained 10 ng pRL-TK. Forty-eight hours after transfection, the dual-luciferase assay was used to detect NF- $\kappa$ B activity. Each value represents the mean  $\pm$  standard deviation from three independent tests. (H) Dose effect on IFN- $\beta$  induction by dual-luciferase assay. The increased doses of either poly(I:C) or M were cotransfected with the pGL3-IFN- $\beta$ -luciferase reporter (100 ng) plus pRL-TK (10 ng) into HEK293T cells. After 48 h of transfection, the dual-luciferase assay was performed to detect IFN- $\beta$  expression. Each value represents the mean  $\pm$  standard deviation from three independent tests. \*,  $P \leq 0.05$ ; \*\*,  $P \leq 0.01$ . (I) Time course effect on IFN- $\beta$  induction examined by dual-luciferase assay. Myc (2  $\mu$ g), M (2  $\mu$ g), and poly(I:C) (2  $\mu$ g/ml) were individually cotransfected with pGL3-IFN- $\beta$ -luciferase reporter (100 ng) plus pRL-TK (10 ng) into

(Continued)

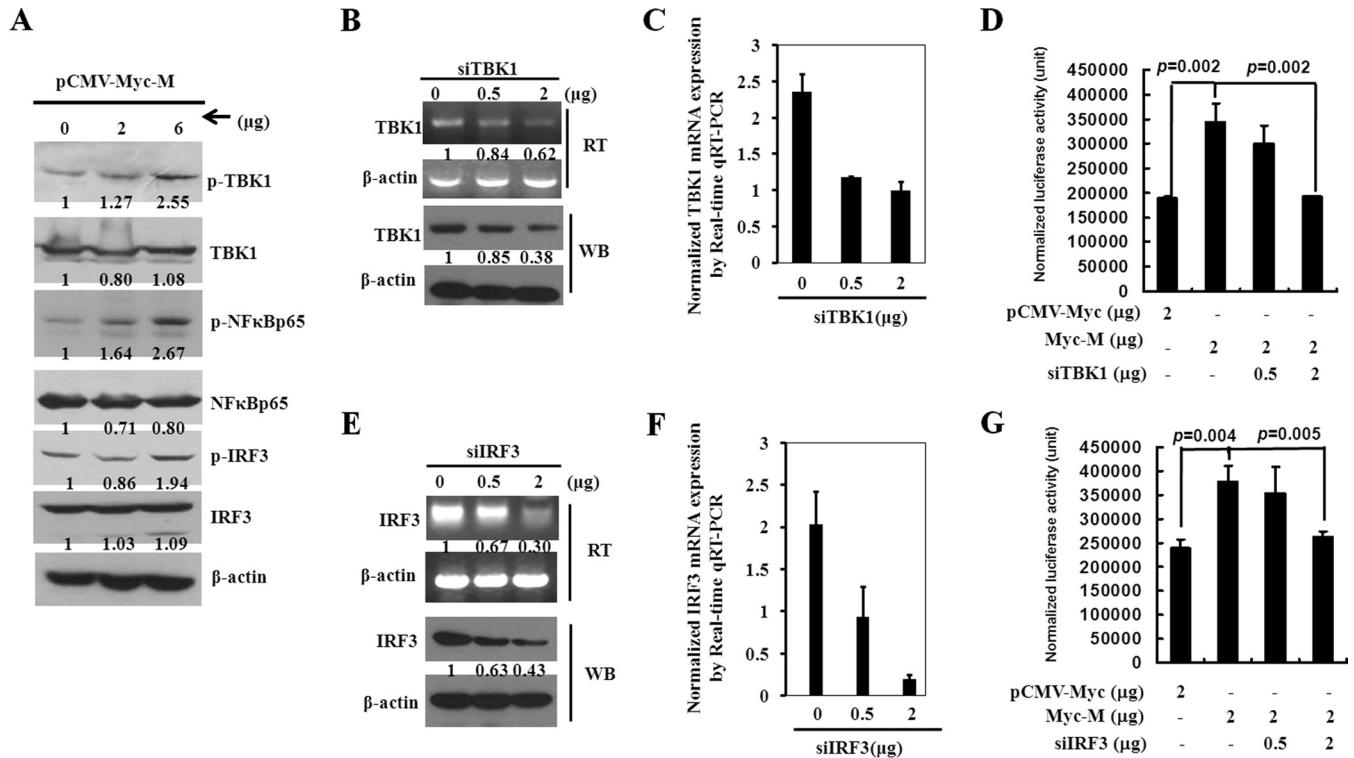


**FIG 2** The SARS-CoV M gene product significantly activated both TBK1-IRF3 and NF- $\kappa$ B signaling pathways and functions at the upstream of TBK1 in HEK293ET cells. (A) Western blotting on M-mediated IFN- $\beta$  and NF- $\kappa$ B activation. The increased doses of pCMV-Myc-M plasmid DNAs (0, 2, and 6  $\mu$ g) were transiently transfected into HEK293ET cells grown on 35-mm<sup>2</sup> culture dishes. Cell lysates were harvested 48 h posttransfection. The reaction products were probed with antibodies to p-TBK1, TBK1, p-NF- $\kappa$ B p65, NF- $\kappa$ B p65, p-IRF3, and IRF3. The expression of  $\beta$ -actin served as a loading control. The relative band intensity was quantitated with the Image J program in comparison with the  $\beta$ -actin control. The result is representative of at least 2 identical experiments. (B) The effect of TBK1 siRNA (siTBK1) on the expression of endogenous TBK1 by semiquantitative RT-PCR. The increased doses of pBS/U6-siTBK1 plasmid DNAs (0, 0.5, and 2  $\mu$ g) were transiently transfected into HEK293ET cells. Total RNAs or whole-cell lysates were isolated or harvested at 48 h posttransfection. One-step RT-PCR (RT) was conducted to detect the TBK1 mRNA expression with specific primers (upper panel), while Western blotting (WB) was performed to detect TBK1 protein expression using specific anti-TBK1 antibody (lower panel). The expression of  $\beta$ -actin served as a loading control. The relative band intensity was quantitated with the Image J program in comparison with the  $\beta$ -actin control. The result is representative of at least 2 identical experiments. (C) Effect of siTBK1 on the expression of TBK1 mRNAs by real-time qRT-PCR analysis. Total RNAs isolated in panel B were subjected to qRT-PCR analysis using specific TBK1 primers. Each value represents the mean  $\pm$  standard deviation from three reactions. The result is representative of at least 2 identical experiments. (D) Effect of siTBK1 on M-mediated IFN- $\beta$  induction. Plasmid pGL3-IFN- $\beta$ -luc reporter was cotransfected with 2  $\mu$ g of pCMV-Myc-M or 2  $\mu$ g of pCMV-Myc-M plus increased doses of siTBK1 (0, 0.5, and 2  $\mu$ g) into HEK293ET cells grown on a 12-well plate. At 48 h posttransfection, the dual-luciferase assay was conducted to assay fold induction of M-mediated IFN- $\beta$  expression. Each value represents the mean  $\pm$  standard deviation from three independent tests. (E) Effect of IRF3 siRNA (siIRF3) on expression of endogenous IRF3 by semiquantitative RT-PCR. The increased doses of pBS/U6-siIRF3 plasmid DNAs (0, 0.5, and 2  $\mu$ g) were transiently transfected into HEK293T cells. Total RNAs or whole-cell lysates were isolated or harvested at 48 h posttransfection. One-step RT-PCR was conducted to detect IRF3 expression with specific primers (upper panel), while Western blotting was performed to detect IRF3 protein expression (lower panel). The expression of  $\beta$ -actin served as a loading control. The result is representative of at least 2 identical experiments. (F) Effect of siIRF3 on M-mediated IFN- $\beta$  mRNA expression by real-time qRT-PCR analysis. Real-time qRT-PCR was performed to detect the IRF3 mRNA (isolated in panel E) expression. Each value represents the mean  $\pm$  standard deviation from three reactions. The result is representative of at least 2 identical experiments. (G) Effect of siIRF3 on M-mediated IFN- $\beta$  induction by luciferase assay. Plasmid pGL3-IFN- $\beta$ -luc reporter was cotransfected with 2  $\mu$ g of pCMV-Myc-M or 2  $\mu$ g of pCMV-Myc-M plus increased doses of siIRF3 (0, 0.5, and 2  $\mu$ g) into HEK293ET cells grown on a 12-well plate. At 48 h posttransfection, the dual-luciferase assay was conducted to assay fold induction of M-mediated IFN- $\beta$  expression. Each value represents the mean  $\pm$  standard deviation from three independent tests.

IRF3, indicating that M gene products may stimulate IFN- $\beta$  activation by promoting its enhanceosome activity. To further define the activation level of M-mediated IFN- $\beta$  induction, specific siRNAs that selectively targeted either TBK1 (Fig. 2B and C) or IRF3 (Fig. 2E and F) mRNAs were generated. Individually diminishing either TBK1 or IRF3 mRNA expression by siTBK1 or siIRF3 sig-

nificantly reversed M-mediated IFN- $\beta$  induction (Fig. 2D and G, respectively), indicating that M-mediated IFN- $\beta$  induction functions at a level at or above the signaling molecule TBK1.

**The SARS-CoV M gene product preferentially activates IFN- $\beta$  production through Toll-like-receptor-related signaling pathways in HEK293ET cells.** RLR and TLR are two main PRRs

#### Figure Legend Continued

HEK293T cells. After 0, 6, 12, and 24 h of transfection, dual-luciferase assays were performed to detect IFN- $\beta$  expression. Each value represents the mean  $\pm$  standard deviation from three independent tests. \*,  $P \leq 0.05$ ; \*\*,  $P \leq 0.01$ . In all data presented above, the relative luciferase activity was determined as firefly luciferase activity divided by *Renilla* luciferase activity.

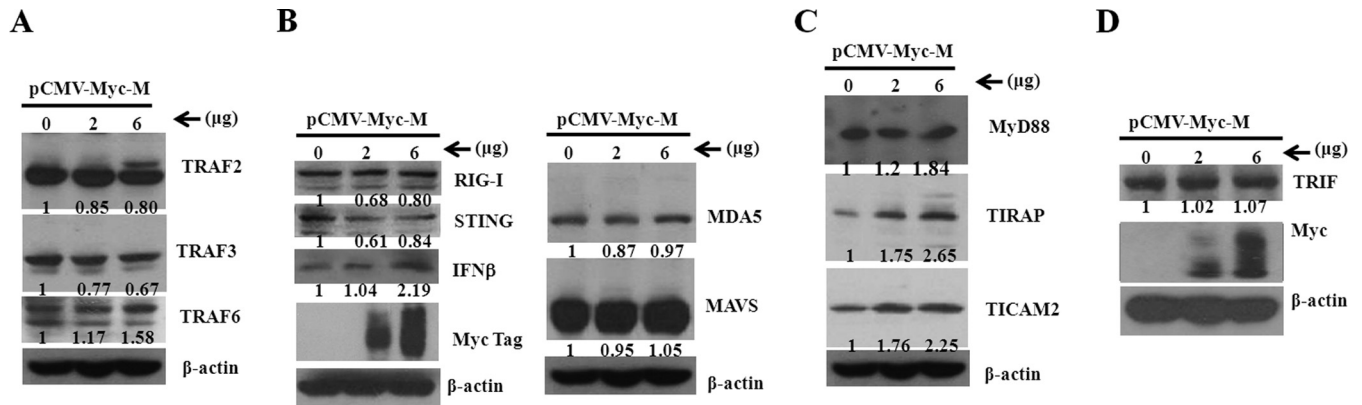


**FIG 3** The influence of the SARS-CoV M gene product on RLR or TLR signaling pathways in HEK293ET cells was assayed by Western blot analysis. (A) Effect of M gene product on expression of TRAF signaling molecules. Cell lysates were prepared from HEK293ET cells that were transiently transfected with increased doses (0, 2, and 6  $\mu$ g) of pCMV-Myc-M for 48 h. The reaction products were probed with anti-TRAF2, anti-TRAF3, and anti-TRAF6. The expression of  $\beta$ -actin served as an internal control. The relative band intensity was quantitated with the Image J program in comparison with the  $\beta$ -actin control. (B) The M gene product did not alter the expression of signaling molecules in the RLR signaling pathway. The reaction products described in panel A were probed with anti-RIG-I, anti-STING, anti-IFN- $\beta$ , anti-Myc tag, anti-MDA5, and anti-MAVS. The expression of  $\beta$ -actin served as an internal control. The relative band intensity was quantitated with the Image J program in comparison with the  $\beta$ -actin control. (C) The M gene product upregulated the expression of adaptor proteins in the TLR signaling pathway. The reaction products described in panel A were probed with anti-MyD88, anti-TIRAP, and anti-TICAM2. The expression of  $\beta$ -actin served as an internal control. The relative band intensity was quantitated with the Image J program in comparison with the  $\beta$ -actin control. (D) The M gene product did not alter the expression of the adaptor protein TRIF. Cell lysates were prepared from HEK293T cells that were transiently transfected with increased doses (0, 2, and 6  $\mu$ g) of pCMV-Myc-M for 48 h. The reaction products were probed with anti-TRIF antibody. The expression of  $\beta$ -actin served as a loading control. The relative band intensity was quantitated with the Image J program in comparison with the  $\beta$ -actin control. Each result is representative of at least 2 identical experiments.

recognizing the majority of extracellular and intracellular PAMPs. Upon the ligation of a PRR with its specific PAMP, both RLR and TLR pathways transmit the signal to a common class of adaptors called tumor necrosis factor (TNF) receptor-associated factors (TRAFs) including TRAF2/TRAF5, TRAF3, and TRAF6 (28, 29). To test the effect of M on RLR and TLR signaling as well as TRAF expression, an increased dose of pCMV-Myc-M constructs was first transiently transfected into HEK293ET cells. The results in Fig. 3A demonstrate that the increased delivery of pCMV-Myc-M into HEK293ET cells markedly enhanced TRAF6 but not TRAF2 and TRAF3 expression, indicating that TRAF6-mediated signaling transduction might contribute to the upregulation of IFN- $\beta$  production. To further address how TRAF expression is associated with RLR and/or TLR signaling pathways, the M gene-transfected HEK293ET cells were also assayed for the expression of upstream sensors and/or signaling molecules of TRAFs. Figure 3B demonstrates that no significant alteration was observed in the expression of RIG-I, MDA5, and MAVS after exogenously delivering M genes into HEK293ET cells, indicating that the RLR signaling pathway might not be targeted by M gene products. In contrast, three adaptor proteins (MyD88, TRAM/TICAM2, and TIRAP) associated with TLRs were all upregulated (Fig. 3C), while the adaptor protein TRIF failed to be upregulated in responding to M gene overexpression (Fig. 3D). Overall, the results indicate that TLR signaling pathways are mainly targeted by the SARS-CoV M gene product for the induction of IFN- $\beta$  expression.

**The SARS-CoV M gene product promotes IFN- $\beta$  production through Toll-like-receptor-related signaling pathways in immortalized murine bone marrow-derived macrophage cells.** To further confirm the above results, the pCMV-Myc-M construct was also transiently transfected into J2-M $\phi$  cells, an immortalized murine bone marrow-derived macrophage cell line established with J2 virus (30, 31). The delivery of the M gene product is effective

in stimulating the activation of both IFN- $\beta$  and NF- $\kappa$ B in murine J2-M $\phi$  cells (Fig. 4A, B, and C). Figure 4D demonstrates that increased delivery of M gene product into J2-M $\phi$  cells indeed promotes IFN- $\beta$  induction through the phosphorylation of IRF3, NF- $\kappa$ B p65, and TBK1. In accord with the results in HEK293ET cells, the increased delivery of pCMV-Myc-M into J2-M $\phi$  cells markedly enhanced TRAF6 but not TRAF2 and TRAF3 expression (Fig. 4E). Moreover, the M gene product did not significantly increase the protein levels of RIG-I, MAVS, STING, and MDA5 (Fig. 4F), indicating that the RIG-I signaling pathway might not be activated in responding to exogenous delivery of the M gene product into J2-M $\phi$  cells. In contrast, the increased delivery of the M gene into J2-M $\phi$  cells markedly enhanced MyD88 and TRAM/TICAM2 but not TRIF expression (Fig. 4G), indicating that TLR-related signaling pathways might be mainly associated with M-mediated IFN- $\beta$  induction. Overall, our data in both HEK293ET and J2-M $\phi$  cells strongly indicate that M-mediated induction of IFN- $\beta$  expression is likely associated with the activation of TLR-related signaling pathways.

**The SARS-CoV M gene product functions at the protein level to induce IFN- $\beta$  production.** The next question that we tried to ask was at which level (mRNA or protein) the M-mediated IFN- $\beta$  induction occurred. To address this issue directly, we created an M-stop construct by replacing the start codon AUG with three in-frame tandem stop codons at the 5' end of the M gene (Fig. 5A). This expression construct can generate only mRNA and no protein due to the translation failure of the mRNA substrates. Western blot analysis shows that the M protein synthesis was completely blocked in the M-stop construct but not the wild-type M construct (Fig. 5B). Real-time quantitative reverse transcription PCR (qRT-PCR) analysis shows that the M-stop construct did not induce IFN- $\beta$  production in HEK293T cells, indicating that

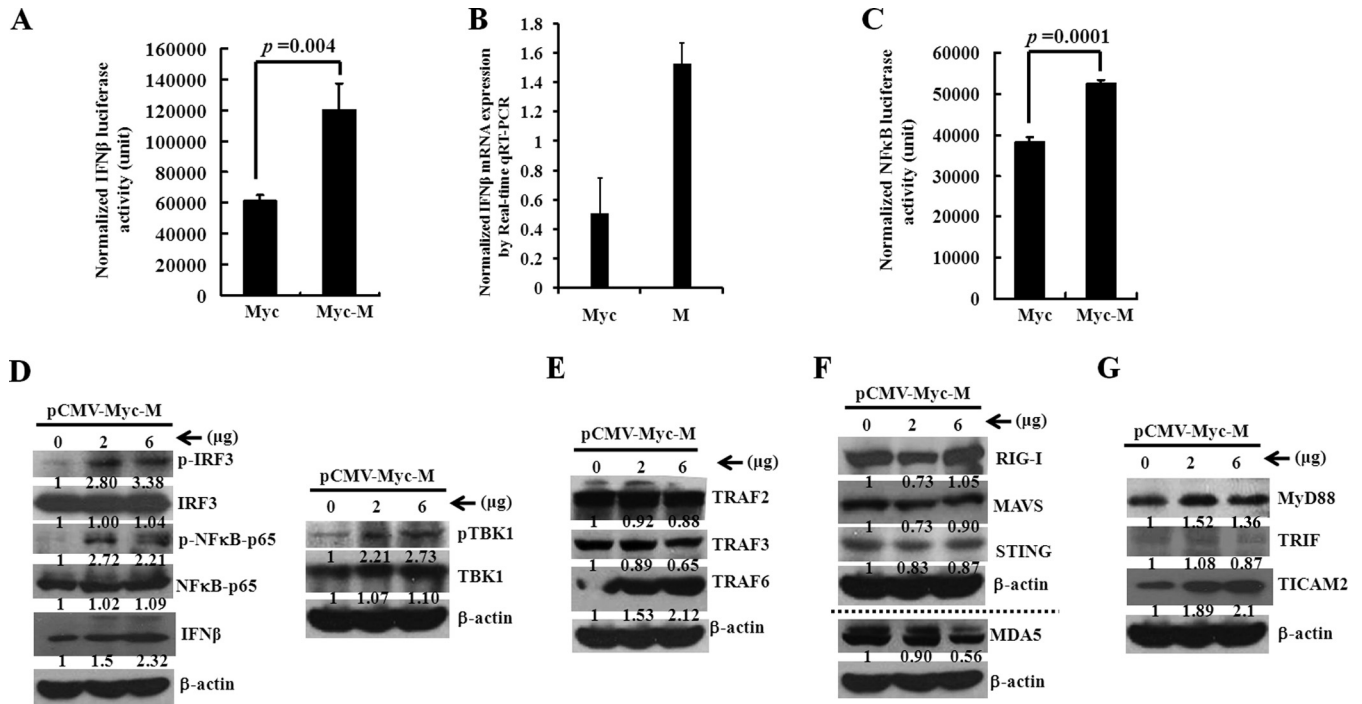


**FIG 4** The effects of the SARS-CoV M gene product on RLR or TLR signaling pathways were assayed in immortalized mouse macrophage J2-M $\phi$  cells. (A) Dual-luciferase analysis of M-mediated IFN- $\beta$  activation. About 100 ng of pGL3-IFN- $\beta$ -luc reporter was cotransfected with 2  $\mu$ g of pCMV-Myc or pCMV-Myc-M plus 10 ng of pRL-TK into J2-M $\phi$  cells. The dual-luciferase assay was conducted to assay the relative expression of the IFN- $\beta$  promoter. Each value represents the mean  $\pm$  standard deviation from three independent tests. (B) Real-time qRT-PCR analysis on M-mediated IFN- $\beta$  gene expression. Total RNAs were isolated from pCMV-Myc- or pCMV-Myc-M-transfected J2-M $\phi$  cells. Real-time qRT-PCR was performed to detect IFN- $\beta$  mRNA expression. The IFN- $\beta$  mRNA level was normalized by using  $\beta$ -actin mRNA as an internal control. Each value represents the mean  $\pm$  standard deviation from three reactions. (C) The M gene product activates the NF- $\kappa$ B signaling pathway. About 100 ng of pNF- $\kappa$ B-luc reporter was cotransfected with 2  $\mu$ g of pCMV-Myc or pCMV-Myc-M plus 10 ng of pRL-TK into J2-M $\phi$  cells. The dual-luciferase assay was conducted to assay the relative expression of the NF- $\kappa$ B promoter. Each value represents the mean  $\pm$  standard deviation from three independent tests. (D) The M gene product activated the downstream signaling molecules of both IFN- $\beta$  and NF- $\kappa$ B signaling pathways. The increased doses of pCMV-Myc-M plasmid DNAs (0, 2, and 6  $\mu$ g) were transiently transfected into J2-M $\phi$  cells. Cell lysates were harvested 48 h posttransfection. The reaction products were probed with antibodies to p-IRF3 and IRF3, p-NF- $\kappa$ B p65 and NF- $\kappa$ B p65, and p-TBK and TBK1. The expression of  $\beta$ -actin served as a loading control. The relative band intensity was quantitated with the Image J program in comparison with the  $\beta$ -actin control. (E) Effects of M gene product on expression of TRAF signaling molecules in J2-M $\phi$  cells. The reaction products described in panel A were probed with anti-TRAF2, anti-TRAF3, and anti-TRAF6. The expression of  $\beta$ -actin served as an internal control. The relative band intensity was quantitated with the Image J program in comparison with the  $\beta$ -actin control. (F) The M gene product did not alter the expression of the signaling molecules in the RLR signaling pathway. J2 wild-type (WT) macrophage cells were transiently transfected with increased doses (0, 2, and 6  $\mu$ g) of pCMV-Myc-M plasmid DNAs. The cell lysates were harvested 48 h posttransfection. The reaction products were probed with anti-MDA5 and anti-MAVS. The expression of  $\beta$ -actin served as an internal control. The relative band intensity was quantitated with the Image J program in comparison with the  $\beta$ -actin control. (G) The M gene product upregulated the expression of adaptor molecules of the TLR signaling pathway. J2-M $\phi$  cells were transiently transfected with the increased doses (0, 2, and 6  $\mu$ g) of pCMV-Myc-M plasmid DNAs. The reaction products described in panel A were probed with anti-MyD88, anti-TRIF, and anti-TICAM2 antibodies. The expression of  $\beta$ -actin served as an internal control. The relative band intensity was quantitated with the Image J program in comparison with the  $\beta$ -actin control. The results in panels D to G are representative of at least 2 identical experiments.

M-mediated IFN- $\beta$  production is dependent on M protein rather than M mRNA (Fig. 5C).

To directly compare M- and M-stop-induced IFN- $\beta$  production levels, the increased doses of either M or M-stop constructs were cotransfected with IFN- $\beta$  luciferase reporter into HEK293T cells. Figure 5D clearly demonstrates that M-stop does not induce IFN- $\beta$  production, indicating that protein translation is necessary for M-induced IFN- $\beta$  production. To confirm this result further, the chemical inhibitor cycloheximide (CHX) was used to block the protein biosynthesis in transfected HEK293T cells. Figure 5E shows that addition of CHX significantly inhibited and completely blocked M protein synthesis at 5  $\mu$ g/ml and above 20  $\mu$ g/ml, respectively, which are directly correlated with the marked reduction and complete inhibition in IFN- $\beta$  expression, indicating that M protein may function as a PAMP to induce IFN- $\beta$  production.

If M protein indeed functions as a PAMP, blocking M protein synthesis should prevent the M-mediated activation of the IFN- $\beta$  signaling pathway. Figure 5F clearly shows that M-stop reverses the M-mediated upregulation of the adaptor proteins MyD88 and TICAM2/TRAM in the initiating phase of TLR signaling pathways. Moreover, M-stop prevents the activation of the downstream modulator and key effectors of the IFN- $\beta$  signaling pathway, such as TBK1, IRF3, and NF- $\kappa$ B p65, in a dose-dependent manner (Fig. 5F). Thus, blocking M protein translation could prevent M-mediated IFN- $\beta$  induction by inactivating the TLR-related signaling pathway.

**SARS-CoV M protein may function as a novel intracellular PAMP to induce IFN- $\beta$  production.** One critical question remaining to be answered is whether the driving force for M protein-mediated IFN- $\beta$  induction is generated intracellularly or extracellularly. To answer this question directly, the TRAP $\gamma$  gene,

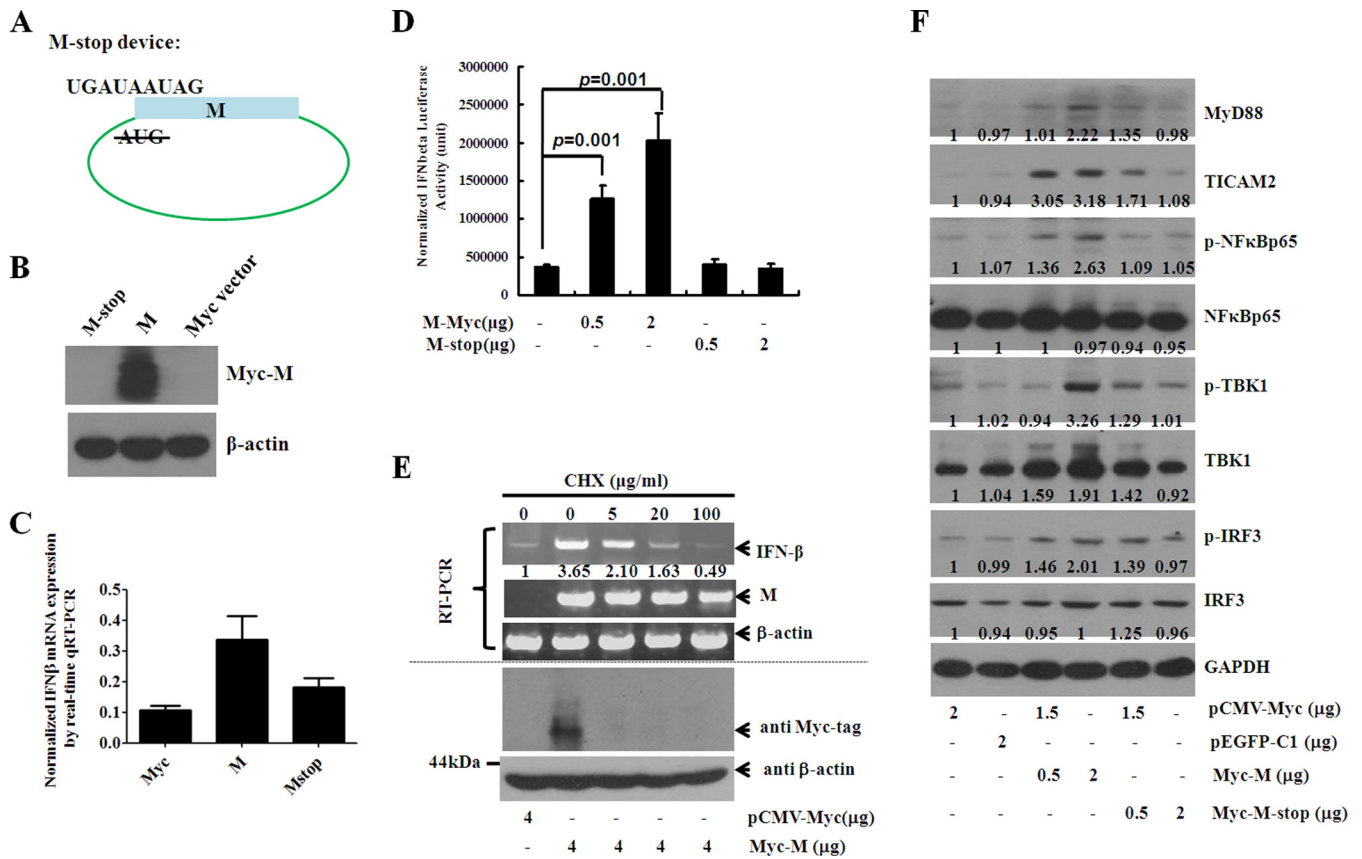


**FIG 5** The SARS-CoV M protein is responsible for the M-mediated IFN- $\beta$  induction. (A) The M-stop construct (pCMV-Myc-M-stop) was created by replacing the AUG initiation codon with three tandem stop codons, UGAUAAUAG, at the 5' end of M cDNA. (B) Western blot analysis of the expression of M and M-stop mutant. About 5  $\mu$ g of pCMV-Myc, pCMV-Myc-M, or pCMV-Myc-M-stop was transiently transfected into HEK293T cells. At 48 h posttransfection, whole-cell lysates were prepared. The reaction products were probed with anti-Myc antibody. The expression of  $\beta$ -actin served as an internal control. The result is representative of at least 3 identical experiments. (C) M-stop failed to induce IFN- $\beta$  expression in HEK293T cells. Total RNAs were isolated from the transfected cells as described in panel B. The reaction products were subjected to real-time qRT-PCR analysis using specific IFN- $\beta$  primers. The IFN- $\beta$  mRNA level was normalized by using  $\beta$ -actin mRNA as an internal control. Each value represents the mean  $\pm$  standard deviation from three reactions. The result is representative of at least 2 identical experiments. (D) M-stop was not able to activate the IFN- $\beta$  promoter activity. The increased doses (0, 0.5, and 2  $\mu$ g) of pCMV-Myc-M or pCMV-Myc-M-stop were transiently cotransfected with 100 ng of pGL3-IFN- $\beta$ -luc plus 10 ng of pRL-TK into a 12-well plate of HEK293T cells. At 48 h posttransfection, cell lysates were prepared. Subsequently, the reaction products were subjected to dual-luciferase analysis. Each value represents the mean  $\pm$  standard deviation from at least three independent tests. (E) M-mediated IFN- $\beta$  induction is translation dependent. HEK293T cells were transiently transfected with 4  $\mu$ g of pCMV-Myc or pCMV-Myc-M. At 2 h posttransfection, the increased doses (0, 5, 20, and 100  $\mu$ g/ml) of cycloheximide (CHX) were added to the culture medium and continuously incubated for 48 h. Both total RNAs and cell lysates were harvested from the same transfection. RT-PCR was conducted to detect the expression levels of IFN- $\beta$ , M gene, and  $\beta$ -actin (panel above the dotted line), while Western blotting was employed to assess the protein expression of both M and the internal control  $\beta$ -actin (panel below the dotted line). The relative band intensity was quantitated with the Image J program in comparison with the  $\beta$ -actin control. The result is representative of at least 2 identical experiments. (F) M-stop inhibited M-mediated IFN- $\beta$  induction. The increased doses (0, 0.5, and 2  $\mu$ g) of either pCMV-Myc-M or pCMV-Myc-M-stop were transiently transfected into HEK293T cells, while transfection with 2  $\mu$ g of either pCMV-Myc or pEGFP-C1 served as a mock control. After 48 h of transfection, cell lysates were subjected to Western blot analysis and probed with anti-MyD88, anti-TICAM2, anti-p-NF- $\kappa$ B p65, anti-NF- $\kappa$ B p65, anti-p-TBK1, anti-TBK1, anti-p-IRF3, and anti-IRF3 antibodies, respectively. The expression of  $\beta$ -actin served as an internal control. The relative band intensity was quantitated with the Image J program in comparison with the glyceraldehyde3-phosphate dehydrogenase (GAPDH) control. The result is representative of at least 2 identical experiments.

an endoplasmic reticulum (ER)-associated gene, was cotransfected with M into HeLa cells. Brefeldin A (BFA) was employed in the assay system to block M protein transport from the rough endoplasmic reticulum to the cell surface. Indeed, the addition of BFA effectively increased the retention of M proteins in the ER compartment (Fig. 6A). Figure 6B shows that addition of BFA also effectively inhibited the secretion of IFN- $\beta$  into the cell culture medium (right panel) but did not inhibit M-mediated IFN- $\beta$  induction at either the mRNA level or the protein level (left panel), indicating that the driving force for M-mediated IFN- $\beta$  induction was indeed derived from intracellular stimulation by M proteins.

Reports indicate that SARS-CoV M protein alone can form virus-like particles (VLPs) that can be secreted extracellularly. Therefore, the secreted M protein might be sensed by its own or other cell PRRs on the cell surface to activate IFN-I responses. To rule out this possibility, OxPAPC (a TLR2 and TLR4 inhibitor) was used to block the function of the accessory proteins CD14, LBP, and MD2 that are required for TLR2 and TLR4 signaling (32). Figure 6C shows that addition of OxPAPC could effectively inhibit lipopolysaccharide (LPS)-mediated IFN- $\beta$  production (right panel) but did not reverse the M-mediated IFN- $\beta$  induction (left panel), indicating that the extracellular stimulation by M pro-

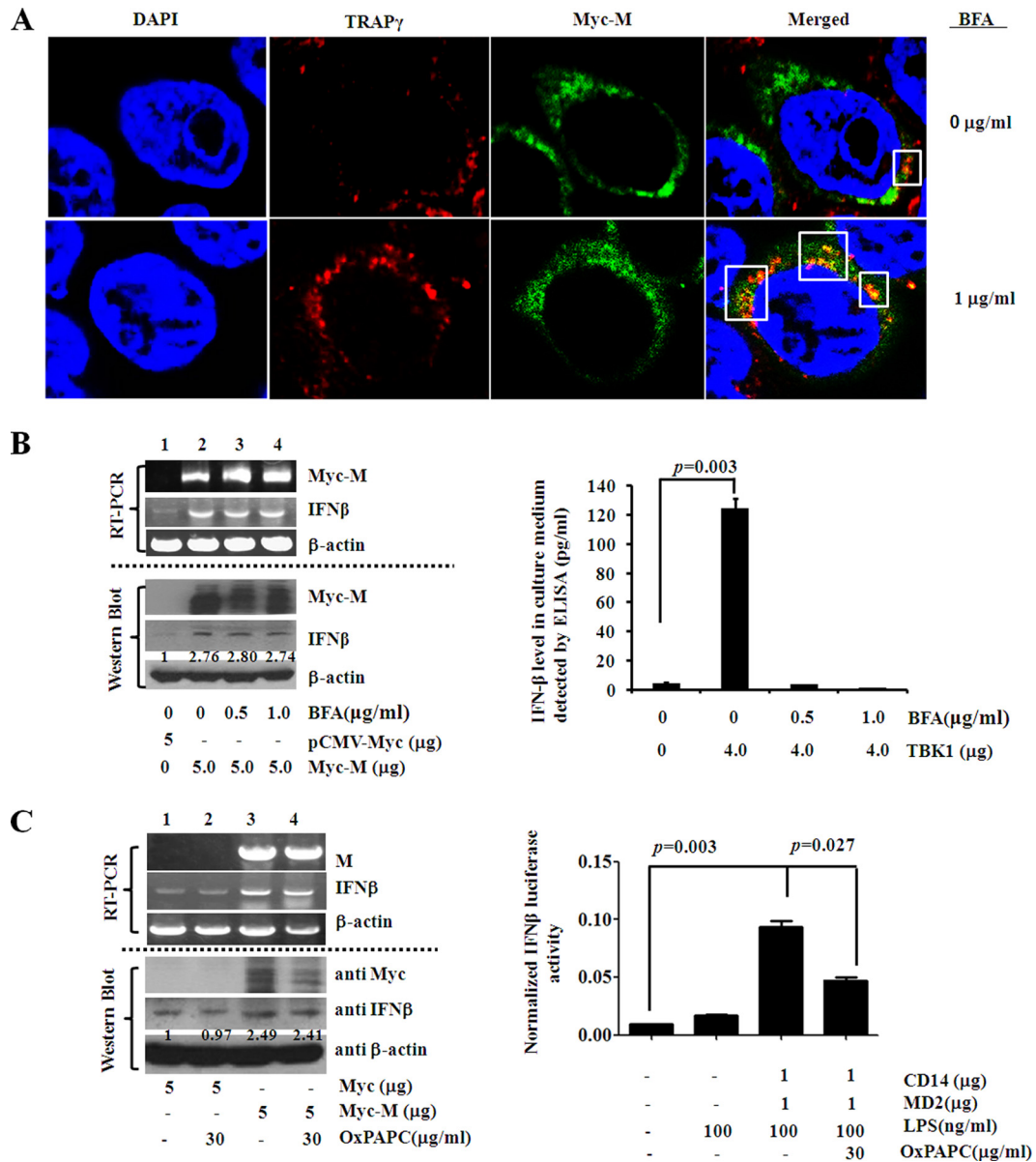


**FIG 6** SARS-CoV M protein functions intracellularly to stimulate IFN- $\beta$  production. (A) Immunostaining analysis on effect of brefeldin A (BFA) on M protein retention in the ER. The gene for ER protein TRAP $\gamma$  was cotransfected with Myc-M into HeLa cells. After probing with a primary antibody to either TRAP $\gamma$  or Myc tag, a fluorescently labeled secondary antibody was applied to the fixed cells. The cell nucleus was stained with DAPI. The immunostained cells were finally subjected to confocal analysis. The empty boxes indicate the colocalization of M and TRAP $\gamma$  in the ER. (B) (Left) The blockade of M protein secretion by BFA did not inhibit M-mediated IFN- $\beta$  production. About 5  $\mu$ g of pCMV-Myc or pCMV-Myc-M was transiently transfected into each 35-mm<sup>2</sup> dish of HEK293T cells. Increased doses of BFA (0, 0.5, and 1.0  $\mu$ g/ml) were added into pCMV-Myc-M-transfected cell medium. Total RNAs and proteins were collected at 48 h posttransfection. RT-PCR analysis was conducted to measure mRNA expression of the IFN- $\beta$  gene in the absence or presence of BFA (above the dotted line). The mRNA expression of the M gene and the loading control of the  $\beta$ -actin gene were also analyzed. In addition, Western blotting was performed to detect the protein expression of IFN- $\beta$  in the absence or presence of BFA (below the dotted line). The expression of M protein and the loading control  $\beta$ -actin was also evaluated. The relative band intensity was quantitated with the Image J program in comparison with the  $\beta$ -actin control. The result is representative of at least 2 identical experiments. (Right) About 4  $\mu$ g of empty vector or pEF-BOS-TBK1 was transiently transfected into each 35-mm<sup>2</sup> dish of HEK293T cells. Increased doses of brefeldin A (0, 0.5, and 1.0  $\mu$ g/ml) were added into pEF-BOS-TBK1-transfected cells. ELISA was used to detect the secreted IFN- $\beta$  in the culture medium, which was downregulated by BFA. (C) (Left) M-mediated IFN- $\beta$  induction is not due to the activation of TLR2 and TLR4 by extracellular M binding. Five micrograms of pCMV-Myc or pCMV-Myc-M was transiently transfected into each 35-mm<sup>2</sup> dish of HEK293T cells. About 30  $\mu$ g/ml of OxPAPC was added into pCMV-Myc- or pCMV-Myc-M-transfected cells. Total RNAs and proteins were collected at 48 h posttransfection. RT-PCR analysis was conducted to measure mRNA levels of IFN- $\beta$  gene expression in the absence or presence of OxPAPC (above the dotted line). The mRNA expression of the M gene and the loading control  $\beta$ -actin gene was also analyzed. In addition, Western blotting was performed to detect the protein expression of IFN- $\beta$  in the absence or presence of OxPAPC (below the dotted line). The expression of M protein and the loading control  $\beta$ -actin was also included. The result is representative of at least 2 identical experiments. (Right) Dual-luciferase assay to detect effect of OxPAPC on LPS-mediated IFN- $\beta$  expression. HEK293T cells were transiently transfected with 100 ng of pGL3-IFN- $\beta$ -luc plus 10 ng of pRL-TK in the absence or presence of 1  $\mu$ g CD14 plus 1  $\mu$ g MD2 plasmids. After 24 h of transfection, the transfected cells were treated with 100 ng/ml LPS or mount control medium in the presence or absence of 30  $\mu$ g/ml OxPAPC for another 24 h. After 48 h of transfection, the dual-luciferase assay was performed to detect the activation of the IFN- $\beta$  promoter. Each value represents the mean  $\pm$  standard deviation from three independent tests.

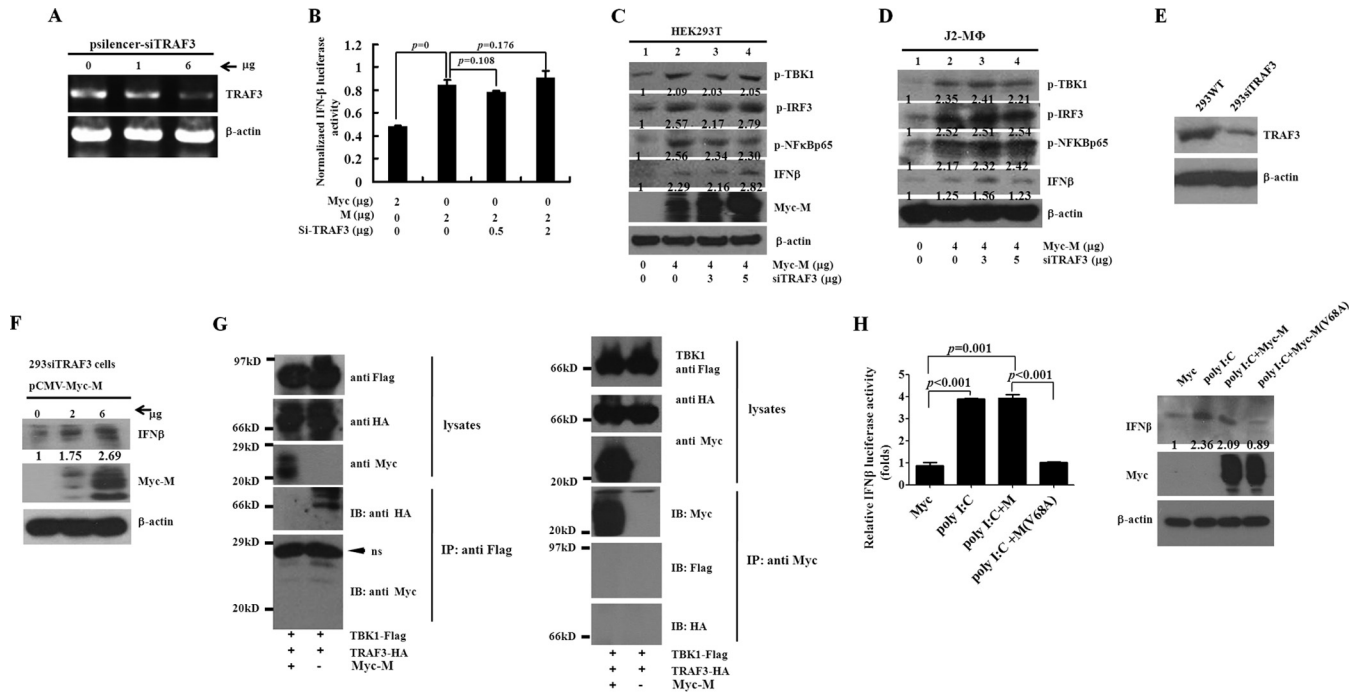


**FIG 7** M protein-mediated IFN- $\beta$  induction is independent of TRAF3. (A) The effect of TRAF3 siRNA (pSilencer-siTRAF3) on the expression of endogenous TRAF3 was evaluated by RT-PCR analysis. The increased doses of pSilencer-siTRAF3 plasmid DNAs (0, 1, and 6  $\mu$ g) were transiently transfected into HEK293T cells. Total RNAs were isolated at 48 h posttransfection. One-step RT-PCR was conducted to detect TRAF3 expression with specific primers. The expression of  $\beta$ -actin served as a loading control. The result is representative of at least 2 identical experiments. (B) The effect of siTRAF3 on M-mediated IFN- $\beta$  induction was evaluated by the dual-luciferase assay. The plasmid pGL3-IFN- $\beta$ -luc reporter was cotransfected with 2  $\mu$ g of pCMV-Myc-M or 2  $\mu$ g of pCMV-Myc-M plus the increased doses of siTRAF3 (0, 0.5, and 2  $\mu$ g) into HEK293T cells. At 48 h posttransfection, the dual-luciferase assay was conducted to assay fold induction of M-mediated IFN- $\beta$  expression. Each value represents the mean  $\pm$  standard deviation from three independent tests. (C) Western blot analysis was conducted to assay the effect of siTRAF3 on the M-mediated IFN- $\beta$  induction in HEK293T cells. Plasmid pCMV-Myc-M was cotransfected with increased doses of siTRAF3 (0, 0.5, and 3  $\mu$ g) into HEK293T cells. Cell lysates were harvested 48 h posttransfection. The reaction products were probed with antibodies to p-TBK1, p-IRF3, p-NF- $\kappa$ B p65, and IFN- $\beta$ . The expression of  $\beta$ -actin served as a loading control. The relative band intensity was quantitated with the Image J program in comparison with the  $\beta$ -actin control. (D) Western blot analysis was conducted to assay the effect of siTRAF3 on the M-mediated IFN- $\beta$  induction in immortalized mouse macrophage J2-M $\phi$  cells. Plasmid pCMV-Myc-M was cotransfected with increased doses of siTRAF3 (0, 0.5, and 3  $\mu$ g) into J2-M $\phi$  cells. Cell lysates were harvested 48 h posttransfection. The reaction products were probed with antibodies to p-TBK1, p-IRF3, p-NF- $\kappa$ B p65, IFN- $\beta$ , and Myc tag. The expression of  $\beta$ -actin served as a loading control. The relative band intensity was quantitated with the Image J program in comparison with the  $\beta$ -actin control. (E) Western blot analysis was conducted to evaluate the expression of TRAF3 in both 293 wild-type and 293 siTRAF3 stable cells. (F) M gene products were able to upregulate IFN- $\beta$  expression after stably knocking down the endogenous TRAF3 expression. Cell lysates were prepared from 293 siTRAF3 stable cells that were transiently transfected with increased doses (0, 2, and 6  $\mu$ g) of pCMV-Myc-M for 48 h. The reaction products were probed with anti-IFN- $\beta$  and anti-Myc antibodies. The expression of  $\beta$ -actin served as an internal control. The relative band intensity was quantitated with the Image J program in comparison with the  $\beta$ -actin control. The result is representative of at least 2 identical experiments. (G) The M gene product may disrupt the TBK1 and TRAF3 complex formation indirectly. Plasmid pCMV-Myc-M or pCMV-Myc was cotransfected with TBK1-Flag and TRAF3-HA. Cell lysates were harvested 48 h posttransfection. Co-IP was conducted as shown in the left panel. About 10% input from each lysate preparation was subjected to Western blot analysis using anti-HA, anti-Flag, and anti-Myc antibodies as probes. The rest of the lysate was first immunoprecipitated with anti-Flag antibody conjugated with an affinity gel. Then, the reaction products were probed with anti-HA and anti-Myc antibodies. A reverse co-IP experiment was also conducted as shown in the right panel. The lysates were first immunoprecipitated with anti-Myc antibody. Then, the reaction products were individually probed with anti-Myc, anti-Flag, and anti-HA antibodies and subsequently subjected to Western blotting. The result is representative of at least 2 identical experiments. IB, immunoblotting; ns, nonspecific. (H) The M gene product does not suppress poly(I:C)-mediated IFN- $\beta$  induction. About 2  $\mu$ g/ml of poly(I:C) was cotransfected with 2  $\mu$ g of either M or M(V68A) plasmid along with pGL3-IFN- $\beta$ -luciferase reporter (100 ng) plus pRL-TK (10 ng) into HEK293T cells. After 48 h of transfection, dual-luciferase assays were performed to detect IFN- $\beta$  expression (left panel). Each value represents the mean  $\pm$  standard deviation from three independent tests. The statistical difference was considered to be significant at a P value of  $\leq 0.05$ . The IFN- $\beta$  expression was also subjected to Western blotting (right panel). The relative band intensity was quantitated with the Image J program in comparison with the  $\beta$ -actin control.

tein may play a marginal role during the activation of IFN- $\beta$  production.

**SARS-CoV M protein promotes IFN- $\beta$  induction independently of TRAF3.** It has been well known that TRAF3 plays a critical role in TLR-mediated IFN- $\beta$  induction, especially through TLR3 and TLR4 pathways (27, 29, 33). Since M protein could activate the TLR pathway from inside the cells, it remained unclear whether or not this activation is in a TRAF3-dependent or -independent manner. To address this issue directly, a specific

siRNA against TRAF3 was successfully constructed (Fig. 7A). A dual-luciferase assay was conducted to assay the effect of siTRAF3 on M-mediated IFN- $\beta$  induction in HEK293T cells. Figure 7B clearly shows that the increased delivery of siTRAF3 did not reverse the M-mediated IFN- $\beta$  induction, indicating that TRAF3 might not be essential for this activation. To further confirm the above result, Western blot analysis was performed to detect IFN- $\beta$  expression in responding to the increased delivery of siTRAF3 into HEK293T cells. The increased delivery of siTRAF3 into HEK293T

cells failed to inactivate the activation of IRF3 and NF- $\kappa$ B p65 and did not affect the M-mediated IFN- $\beta$  induction (Fig. 7C), while a result was obtained consistent with the increased delivery of si-TRAF3 into J2-M $\phi$  cells (Fig. 7D). In addition, a stable HEK293 cell line with TRAF3 knocked down by siTRAF3 was also established (Fig. 7E). A dose-dependent increase in IFN- $\beta$  production was observed with the increased delivery of M gene into 293 si-TRAF3 stable cells (Fig. 7F). Thus, the above data strongly indicate that TRAF3 is not required for M-mediated IFN- $\beta$  induction.

SARS-CoV M protein has been shown to destabilize the functional TRAF3-TBK1 complex formation (34). However, it remains unknown whether or not M protein is able to associate with the key components of this complex. To clarify this issue directly, a coimmunoprecipitation (co-IP) experiment was conducted. Plasmid TBK1-Flag, TRAF3-HA, and Myc-M DNAs were transiently cotransfected into HEK293T cells. The cell lysates were first immunoprecipitated with anti-Flag antibody conjugated with an affinity gel and then subsequently probed with antihemagglutinin (anti-HA) and anti-Myc antibodies. The left panel of Fig. 7G indicates that M protein was able to disrupt the physical interaction between TBK1 and TRAF3, but M protein itself could not form a complex with TBK1. In the reverse immunoprecipitation (IP) experiment as shown in the right panel of Fig. 7G, M protein was unable to interact with both TBK1 and TRAF3 directly, indicating that M protein may modulate the TBK1-TRAF3 complex formation indirectly. Interestingly, in contrast to the inhibitory effect of M(V68A) on poly(I:C)-mediated IFN- $\beta$  induction, the M gene product did not affect the IFN- $\beta$  induction stimulated by poly(I:C) (Fig. 7H), indicating that M has no effect on poly(I:C)-induced IFN- $\beta$  production while retaining the ability to destabilize the complex formation.

**SARS-CoV carrying the M mutant [M(V68A)] fails to activate IFN- $\beta$  production in infected cells.** One critical question remaining to be answered is whether or not M-mediated IFN- $\beta$  induction could occur in real virus infection. It has been shown that codelivering the M, N, and S genes of SARS-CoV into HEK293 cells readily produced SARS-CoV pseudovirus with the corona-like halo (35). Earlier results demonstrate that valine-to-alanine mutation at residue 68 [abbreviated as M(V68A)] inhibited IFN- $\beta$  induction (34). We employed a SARS-CoV pseudovirus system to mimic the real SARS-CoV infection. Cell lysate supernatants isolated from either M, N, and S cotransfection or M(V68A), N, and S cotransfection were first incubated with 293-ACE2 stable cells (Fig. 8A) for 4 h. Then, the cell culture medium was replaced with fresh medium and further incubated at 37°C for another 24 h before harvesting. The SARS-CoV pseudovirus VLP(S-M-N) markedly upregulated IFN- $\beta$  expression at both RNA and protein levels (Fig. 8B), whereas the point mutation at the valine 68 residue of M protein completely diminished SARS-CoV pseudovirus-mediated IFN- $\beta$  induction, strongly indicating that the M protein residing on SARS-CoV virion could specifically induce IFN- $\beta$  production upon infecting the targeted cells. Taken together, our data indicate for the first time that SARS-CoV M protein may function as a novel cytosolic PAMP to activate IFN- $\beta$  induction through an intracellular TLR-related signaling pathway in a TRAF3-independent manner.

## DISCUSSION

Pathogen-associated molecular patterns (PAMPs) are pathogen-borne components that can be sensed by either transmembrane,

endolysosomal, or cytosolic sensors known as pattern recognition receptors (PRRs) (36). In this study, we demonstrate that the membrane protein of SARS-CoV significantly upregulates IFN- $\beta$  production by activating both NF- $\kappa$ B and TBK1-IRF3 signaling cascades. Our data show that M-mediated IFN- $\beta$  production is induced by M protein rather than M mRNA, indicating that pathogen-derived protein might be able to serve as a cytosolic PAMP. In addition, a mechanism study indicates that M protein-mediated IFN- $\beta$  induction may be mainly due to the selective activation of TLR-related signaling pathways rather than the RLR signaling pathway in a TRAF3-independent manner. Overall, the current study indicates for the first time that pathogen-derived protein may function as a novel cytosolic PAMP to initiate a TLR-related TRAF3-independent signaling pathway that subsequently promotes type I interferon (IFN-I) production.

The membrane-associated PRRs, such as TLR2 and TLR4, can sense not only bacterial components but also viral coat proteins (37). Kurt-Jones and colleagues first demonstrated that the innate immune response to the fusion (F) protein of respiratory syncytial virus (RSV) is mediated by TLR4 plus its cofactor CD14 on the plasma membrane, indicating that nonbacterial components can serve as extracellular PAMPs (24). Although some viral structural proteins, such as the nucleocapsid (N) from measles virus (38) and viral ribonucleoprotein from vesicular stomatitis virus (39), can activate IRF3 and TBK1/IKK $\delta$ , respectively, it remains to be determined how these viral products can function as PAMPs and where the driving forces for their activation come from. It has been shown that the SARS-CoV M protein alone not only can form virus-like particles (VLPs) in a viral RNA-independent manner (40) but also can induce cell apoptosis by inhibiting some key survival signal pathways, such as the Akt signaling pathway (41). Thus, the M proteins derived from these infected and apoptotic cells might be eventually secreted and released into the extracellular compartments where the TLRs (such as TLR2 and TLR4) on the cell surface can be potentially recognized and subsequently activated by these extracellular PAMPs for the induction of the IFN-I response. To clarify this possibility, we employed several approaches to test whether the driving force for M protein-mediated IFN- $\beta$  production is generated from inside or outside the cells. We used two types of inhibitors, BFA and OxPAPC, to block either the intracellular transport of M protein or the extracellular binding of M protein on TLR2 and TLR4, respectively. Our results reveal that M-mediated IFN- $\beta$  induction is independent of M protein secretion as well as the extracellular stimulation of TLR2/TLR4 signaling, indicating that the driving force for the M-mediated IFN- $\beta$  induction is likely generated from inside the cells.

Our results may contradict some previous reports related to M-mediated IFN-I response. Siu et al. demonstrated that the M protein of SARS-CoV negatively regulated the dsRNA-induced and signaling molecule-induced IFN-I production. They also showed that M protein alone was unable to activate the IFN-I promoter activity (34). One study even showed that M protein negatively regulates the NF- $\kappa$ B signaling pathway (42). A possible explanation for these discrepancies might be related to the M gene itself. Early study has shown that M protein possesses a higher substitution rate than other structural proteins in SARS-CoV, and the outcome of these substitutions alters the biochemical and immunological properties of M proteins (43, 44). One amino acid alteration from valine to alanine at residue 68 is indeed found in

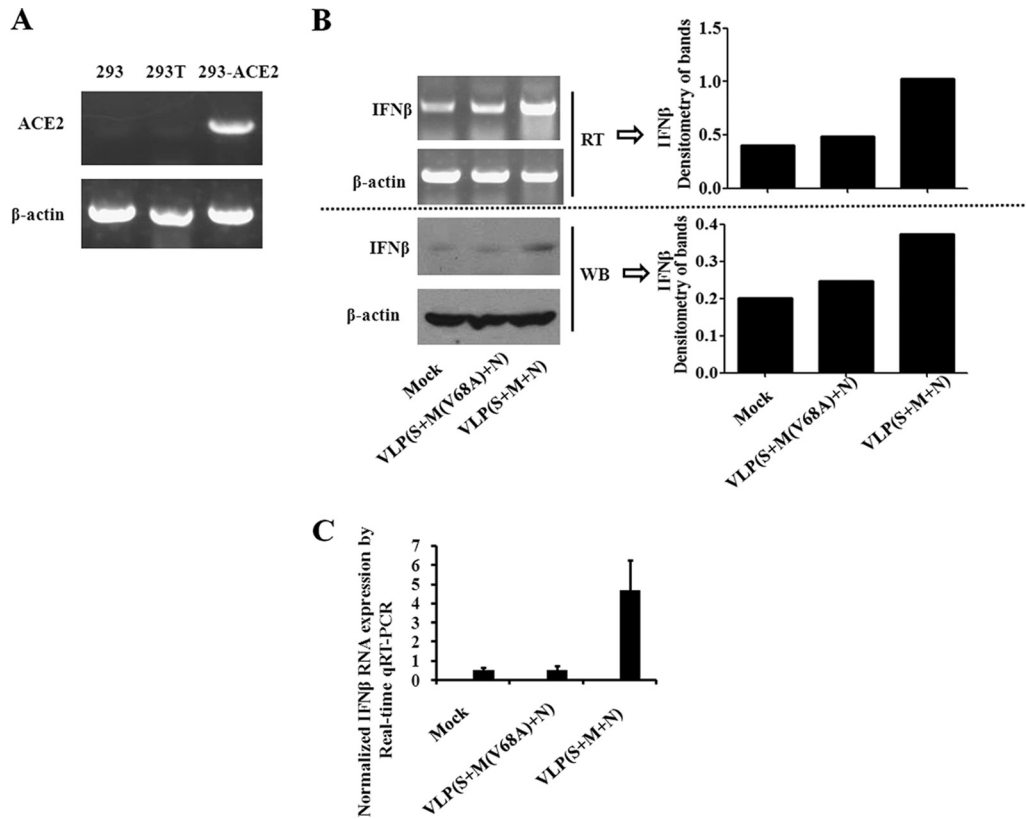


**FIG 8** M protein derived from SARS-CoV pseudoviruses (or virus-like particles [VLPs]) specifically upregulates the IFN- $\beta$  expression. (A) RT-PCR was used to detect the mRNA expression of ACE2 in the HEK293, HEK293T, and HEK293-ACE2 stable cell line. The result is representative of 3 identical experiments. (B) Effect of SARS-CoV pseudoviruses and their M protein mutant derivative on the influence of IFN- $\beta$  expression. Plasmid S and N DNAs were cotransfected with either M mutant M(V68A) or the wild-type M into HEK293T cells. After 48 h of transfection, SARS-CoV VLPs were formed and released by three cycles of freezing and thawing. Then, the collected VLPs were incubated with equal amounts of HEK293-ACE2 cells for 4 h and changed with fresh culture medium. After 24 h, total RNAs and whole-cell lysates were isolated, harvested, and subsequently subjected to RT-PCR (RT; upper panel) and Western blotting (WB; lower panel). The relative band intensity was quantitated with the Image J program in comparison with the  $\beta$ -actin control. The result is representative of at least 2 identical experiments. (C) Effect of both M and M(V68A) VLPs on IFN- $\beta$  expression in HEK293-ACE2 stable cells. Real-time qRT-PCR was used to detect the IFN- $\beta$  mRNA levels on the samples isolated in panel B. Each value represents the mean  $\pm$  standard deviation from three reactions. The result is representative of at least 2 identical experiments.

the M protein from the GZ50 isolate studied by Siu et al. compared with the isolate used in the current study. Our functional analysis provides strong evidence to demonstrate that the valine-to-alanine change at residue 68 of M protein is sufficient to abolish M-mediated IFN- $\beta$  induction at both the transient-transfection level and the viral infection level (Fig. 1D and E and 8B and C). Therefore, this amino acid substitution in M proteins indeed affects the interaction between M protein and the PRR for the subsequent IFN-I induction.

It still remains elusive which cytosolic PRR is responsible for M-mediated IFN- $\beta$  induction. The M protein might be a multifaceted molecule that physically interacts with diverse intracellular sensors and signaling factors (34, 42). Our data indicate that the TLR-related signaling pathway rather than the RIG-I signaling cascade is responsible for M-mediated IFN- $\beta$  induction. Interestingly, we observed consistent TRAF3 reductions in both HEK293T and J2-M $\phi$  cells as tested by the transiently intracellular overexpression of the M gene. TRAF3 is one of the key signaling molecules specifically responsible for IFN-I induction (28). Data from the work of Siu and colleagues have shown that M(V68A) excludes the TRAF3 inclusion in the TRAF3.TANK.TBK1/IKK $\epsilon$

complex (39). Although M(V68A)-mediated TRAF3 exclusion inhibits IFN- $\beta$  induction, our study showed that M-mediated TRAF3 exclusion is independent of ligand stimulation and the disassociated TRAF3 and TBK1 could not complex with M protein, indicating that M protein might modulate the functions of TBK1 complex indirectly. Interestingly, we demonstrated that M-mediated IFN- $\beta$  induction was associated with the upregulation of the adaptor proteins MyD88, TIRAP, and TICAM2 but not TRIF, which are all involved in the initiating phase of TLR signaling pathways. TRIF is required for both TLR3- and TLR4-mediated IFN- $\beta$  induction. In the activation of TLR3, TRIF is directly recruited to the TIR domain of dimerized TLR3, while in the activation of TLR4, TRIF is recruited to dimerized TLR4 indirectly through another TIR-containing adaptor protein, TICAM2 (also called TRAM). If TRIF is not required for M-mediated IFN- $\beta$  induction, M-mediated IFN- $\beta$  induction might be activated via a noncanonical TLR4-related signaling cascade independently of TRIF and TRAF3.

In summary, the current study demonstrates for the first time that the M protein of SARS-CoV is able to function as a cytosolic PAMP to promote IFN- $\beta$  production by activating a TLR-related

TABLE 1 Primers used in RT-PCR analysis

Gene name	GenBank ID	Forward primer (5'-3')	Reverse primer (5'-3')	Size of product (bp)
<i>IRF3<sup>a</sup></i>	NM_001571	AAGGACAAGGAAGGAGGCGT	AGAGTGGGTGGCTGTTGGAA	283
<i>TRAF3</i>	NM_00119942.7	GCGTGCAGAGAGCATCGT	CTTGGCTGTCTATCACTCGCT	462
<i>TBK1<sup>a</sup></i>	NM_013254	ATCACTGCCCTTAGACCCCT	TGGTATTCAGAGGTTCCCG	518
<i>IFN<math>\beta</math><sup>a</sup></i>	NM_002176	ATGACCAACAAGTGTCTCCT	TTCAGTTTCGGAGGTAACCT	564
<i>SARS-M</i>	AY278491	TATAGAATTCTGGCAGACAACGGTACTATT	TATAGGTACCGTCACTTACTGTACTAGCAAAGC	686
<i><math>\beta</math>-actin<sup>a</sup></i>	BC009275	CACACTGTGCCATCTACGA	CTGCTTGTGATCCACATCT	600
<i><math>\beta</math>-actin<sup>b</sup></i>	BC009275	TCCATCATGAAGTGTGACGT	CTCAGGAGGAGCAATGATCT	161
<i>IFN<math>\beta</math><sup>b</sup></i>	NM_002176	ATGACCAACAAGTGTCTCCT	CTGTCTTGAGGCAGTATTC	176
<i>TBK1<sup>b</sup></i>	NM_013254	GACGAACCGCACCACTGTTA	GATCTGGGCACCTTGAAAAATAAATA	86
<i>IRF3<sup>b</sup></i>	NM_001571	AAGGACAAGGAAGGAGGCGT	CGAGCCTCTTGGTCCACGGC	151

<sup>a</sup> Primer for standard RT-PCR.

<sup>b</sup> Primer for real-time quantitative RT-PCR.

TRAF3-independent pathway. The driving force for M-mediated IFN- $\beta$  induction is likely generated from inside the cells rather than the extracellular binding of M proteins with the defined cell surface PRRs, such as TLR4.

## MATERIALS AND METHODS

**Cell lines and reagents.** Human embryonic kidney cell line 293T (HEK293T) and 293ET (HEK293ET) cells were obtained from the Cell Culture Center of the Institute of Basic Medical Sciences, Chinese Academy of Medical Sciences. The HEK293T cell line was transformed with the simian virus 40 (SV40) large T antigen, while the HEK293ET cell line was transformed with both SV40 large T antigen and EBNA1 antigen. Cells were cultured in Dulbecco's modified Eagle's medium (Life Technologies, Grand Island, NY) supplemented with 10% fetal calf serum and incubated in a 37°C incubator with 5% CO<sub>2</sub>. J2-M $\phi$  cells were a gift from Genhong Cheng and were cultured in RPMI 1640 (Life Technologies, Grand Island, NY, USA) supplemented with 10% fetal calf serum and incubated in a 37°C incubator with 5% CO<sub>2</sub>. Anti-Myc and anti-NF- $\kappa$ B-p65 antibodies were purchased from Santa Cruz Biotechnology (Santa Cruz, CA, USA); anti-TBK1 and anti-pTBK1 were derived from Epitomics (Burlingame, CA, USA); anti-IRF3 and anti-pIRF3 were purchased from Anbo Biotechnology (Changzhou, Jiangsu, China); anti-pNF- $\kappa$ B-p65, anti-TRAF3, and anti-TRAF6 were from Bioworld Technology, Inc. (St. Louis Park, MN, USA); anti-RIG-I (DDX58), anti-MDA5 (IFIHI), and anti-MAVS were obtained from Proteintech Group, Inc. (Chicago, IL, USA); anti-TRAF2 was purchased from Bioss Biotechnology (Beijing, China); and anti-TICAM1 was from Affinity (Ohio, USA). Plasmid pNF- $\kappa$ B-luc was derived from Stratagene (La Jolla, CA, USA). Plasmid pRL-TK was obtained from Promega (Madison, WI, USA). Plasmid pSilencer 4.1-CMV neo was from Thermo Scientific (Waltham, MA, USA). Both pEF-BOS-TBK1 and pCDNA-HA-TRAF3 were from Addgene (Cambridge, MA, USA).

**Plasmid construction.** Plasmids pCMV-Myc-M and pBS-U6-siM1 were constructed previously (26). Plasmids pCMV-Myc-S and pCMV-Myc-E were constructed by inserting S and E into the EcoRI and KpnI sites of pCMV-Myc. The mutant of pCMV-Myc-M(V68A) was generated by using the site-directed mutagenesis kit (TaKaRa, Dalian, China). One copy of the IFN- $\beta$  promoter sequence (5'-CTAAAATGTAAATGACATAGGAAAAGTGAAGGGGAGAAGTGAAGTGGGAAATTCCTCTGAATAGAGAGAGGACCATCTCATATAAATAGGCCATACCCATGGAGAAAGGACATTCTAACTGCAACCTTTCGA-3') was PCR amplified and subcloned into the KpnI and XhoI sites of the luciferase reporter pGL3-basic (Promega, Madison, WI, USA) to generate the pGL3-IFN- $\beta$ -luc construct. All primers were synthesized by Sangon (Shanghai, China). For the construction of pBS/U6 siTBK1, the sense strand 5' TCGAGTTGCGAAGCCGGAAGTGTCTTAAGCTTAGGACACTTCCGGCTTCGCAATTTTG 3' and antisense strand 5' ACGCTTCGGCCTTCACAGGATTCGAATCCTGTGAAGGCCGAAGCGTTAAAAACTTAA 3' were annealed and then subcloned into the EcoRI and XhoI sites of pBS/U6. For the

construction of pBS/U6 siIRF3, the sense strand 5' TCGAGCATCGGCTTTGGGTCTGTAAAGCTTTAAACAGACCCAAAAGCCGATGTTTTTG 3' and antisense strand 5' CGTAGCCGAAAACCCAGACAATTTGAAATTGTCTGGGTTTTTCGGCTACAAAACTTAA 3' were annealed and then subcloned into the EcoRI and XhoI sites of pBS/U6.

For construction of pSilencer-siTRAF3, the single-strand oligonucleotides 5' GATCCGCGAGAAGTCTCTTCCCTCGAGGGAAAAGAGGAGTTCTCGCAGA 3' and 5' AGCTTCTCGAGAAGTCTCTTCCCTCGAGGGAAAAGAGGAGTTCTCGCAGA 3' were annealed to double strands before being subcloned into the HindIII and BamHI sites of pSilencer 4.1-CMV neo to form the pSilencer-siTRAF3 construct.

**Transient transfection.** Cells (HEK293ET, HEK293T, and J2-M $\phi$ ) were transiently transfected with the plasmid DNAs (pCMV-Myc-M, pCMV-Myc, pGL3-IFN- $\beta$ -luc, or pNF- $\kappa$ B-luc) using VigoFect (Vigorous Biotechnology, Beijing, China) according to the manufacturer's instructions. For example, about 5  $\mu$ g plasmid DNAs was first added to 100  $\mu$ l of 0.9% NaCl. Then, 2.5  $\mu$ l VigoFect was resuspended into another 100  $\mu$ l of 0.9% NaCl solution. Then, the DNA-NaCl mixture was added to the VigoFect-NaCl mixture drop by drop with gentle vortexing. After a 15-min incubation at room temperature, the reaction product was evenly distributed onto the cell culture surface of either 6-well plates or 35-mm<sup>2</sup> dishes and then continuously incubated for 48 h before harvesting.

**Construction of the 293 siTRAF3 stable cells.** Plasmid pSilencer-siTRAF3 DNAs (5  $\mu$ g) were transfected into HEK293 cells. After a 24-h transfection, the cell culture medium was replaced with fresh medium containing 1,200  $\mu$ g/ml G418. After 2 weeks of culture, cell colonies were picked up and expanded in a 24-well tissue culture plate. Finally, Western blot analysis was performed to detect TRAF3 expression.

**Reverse transcription-PCR (RT-PCR) and qRT-PCR.** Total RNAs were extracted from the cultured cells with TRIzol (Invitrogen, Carlsbad, CA, USA). The purified total RNAs were treated with DNase I (Qiagen, Düsseldorf, Germany). All primers used in the RT-PCRs are listed in Table 1. The RT-PCR was carried out with the PrimeScript one-step RT-PCR kit (TaKaRa Biotechnology, Dalian, China) according to the manufacturer's instructions. The RT-PCR was carried out in a DNA Thermal Cycler (Applied Biosystems, Carlsbad, CA) under the following conditions: 50°C for 35 min for reverse transcription and 94°C for 5 min for denaturation. The PCR conditions were 94°C for 30 s, 50°C for 30 s, and 72°C for 50 s, repeated for 20 to 30 cycles; the reaction was extended at 72°C for 10 min before the reaction product was stored at 4°C. One-step real-time quantitative RT-PCR (qRT-PCR) (TaKaRa Biotechnology, Dalian, China) was also performed to monitor the targeted gene expression. The primers used in qRT-PCR were also listed in Table 1. Real-time qRT-PCR was carried out with the CFX real-time PCR detection system (Bio-Rad Laboratories, Hercules, CA, USA) under the following conditions: 42°C for 5 min and 95°C for 10 s, and then 95°C for 5 s and 60°C for 10 s, repeated for 40 cycles. The dissociation of the reaction products was conducted from 55°C to 95°C as the temperature rose at 0.2°C per 10 s.

**Western blot analysis.** The transfected cells were lysed with a lysis buffer containing 1% NP-40, 50 mM Tris-HCl (pH 7.5), 120 mM NaCl, 200  $\mu$ M NaVO<sub>4</sub>, 1  $\mu$ g/ml leupeptin, 1  $\mu$ g/ml aprotinin, and 1  $\mu$ M phenylmethylsulfonyl fluoride (PMSF). About 15  $\mu$ g of cell lysate for each sample was resolved by 12% SDS-PAGE. After separation, the reaction products were transferred onto a Hybond nitrocellulose membrane (Pharmacia, St. Louis, MO, USA). The transferred membrane was first probed with a primary antibody. Then, a secondary antibody labeled with horseradish peroxidase was added to the reaction product and was finally visualized with an enhanced chemiluminescence (ECL) kit (Santa Cruz Biotechnology, Santa Cruz, CA, USA).

**Dual-luciferase assay.** The dual-luciferase kit was purchased from Promega (Promega Corporation, USA). Cells were transfected with pGL3-IFN- $\beta$ -luc or pNF- $\kappa$ B-luc plus pRL-TK at the ratio of 100:1 or 10:1 as suggested by the manual. The detection was done by following the assay protocol in the kit. The firefly and *Renilla* luciferase activities were read with a Modulus microplate multimode reader (Turner Biosystems, Sunnyvale, CA, USA).

**Coimmunoprecipitation (co-IP) assay.** The transfected cells were lysed with a lysis buffer containing 50 mM Tris-HCl (pH 7.4), 150 mM NaCl, 1 mM EDTA, 0.2% Triton, 1  $\mu$ g/ml leupeptin, 1  $\mu$ g/ml aprotinin, and 1 mM PMSF. About 10% of the lysate was subjected to input analysis. Flag affinity gel (Sigma, USA) or anti-Myc and protein G plus agarose (Santa Cruz Biotechnology, Santa Cruz, CA, USA) were added to the rest of the lysate (90%) and rotated overnight at 4°C. The reaction products were washed 5 times with a wash buffer and then centrifuged at 5,000 rpm for 1 min. The IP products were resuspended in the loading buffer and subjected to Western blot analysis.

**ELISA.** Cell culture supernatants were harvested 48 h after transfection. The human IFN- $\beta$  ELISA kit was purchased from Bluegene (Shanghai, China). The reaction was carried out by following the manufacturer's instructions. The reaction products were detected with Synogen 4 (BioTek, Seattle, WA, USA) under 450 nm.

**Generation of SARS-CoV pseudovirus and assay of virus-induced IFN- $\beta$  production.** The generation of SARS-CoV pseudovirus followed the procedure described by Huang et al. (35). Briefly, HEK293 cells were cotransfected with either the S, M, and N genes or the S, M mutant M(V68A), and N of SARS-CoV. After 48 h of transfection, the culture medium and the transfected cells were collected and subjected to freezing and thawing cycles at least four times. The reaction products were centrifuged at 12,000 rpm for 10 min. The supernatant containing VLPs was then applied to HEK293-ACE2 stable cells and incubated for 4 h. Then, the cell culture medium was replaced with fresh medium. After 24 h, the infected cells were subjected to total RNA isolation and preparation of whole-cell lysates as described elsewhere. SARS-CoV-mediated IFN- $\beta$  expression was monitored by standard Western blotting, RT-PCR, and qRT-PCR.

**Immunostaining assay.** HeLa cells were transiently transfected with Myc-M and Flag-TRAP $\gamma$  (45). After 24 h of transfection, the cells were fixed with 4% formaldehyde for 20 min on ice and then incubated in 1 $\times$  phosphate-buffered saline (PBS) containing 10% bovine serum albumin (BSA) for 1 h. The cells were first incubated with primary antibody rabbit anti-Flag or mouse anti-Myc for 1 h. Then, the secondary antibody fluorescein isothiocyanate (FITC)-labeled goat anti-mouse or tetramethyl rhodamine isocyanate (TRITC)-labeled goat anti-rabbit antibody was added, and the mixture was incubated for another 1 h. Finally, the cells were incubated with 4',6-diamidino-2-phenylindole (DAPI) and sealed with glycerol. The results were observed under an Olympus FV1000 confocal microscope.

**Statistical analysis.** All values were calculated as means  $\pm$  standard deviations (SDs) from three independent experiments. The statistical difference between the assayed group and the standard group was subjected to Student's *t* test. The calculated difference was considered significant at the *P* value of <0.05.

## ACKNOWLEDGMENTS

We thank Genhong Cheng and Hang-Zi Chen for providing the J2-M $\phi$  cells and TRAP $\gamma$ , respectively.

## FUNDING INFORMATION

National Natural Science Foundation of China (NSFC) provided funding to Li Liu under grant number 30871283. National Natural Science Foundation of China (NSFC) provided funding to Li Liu under grant number 81171944. National Natural Science Foundation of China (NSFC) provided funding to Li Liu under grant number 81550030.

## REFERENCES

- Bowie AG, Unterholzner L. 2008. Viral evasion and subversion of pattern-recognition receptor signalling. *Nat Rev Immunol* 8:911–922. <http://dx.doi.org/10.1038/nri2436>.
- Nagarajan U. 2011. Induction and function of IFN $\beta$  during viral and bacterial infection. *Crit Rev Immunol* 31:459–474. <http://dx.doi.org/10.1615/CritRevImmunol.v31.i6.20>.
- Takeuchi O, Akira S. 2009. Innate immunity to virus infection. *Immunol Rev* 227:75–86. <http://dx.doi.org/10.1111/j.1600-065X.2008.00737.x>.
- Yamamoto M, Sato S, Hemmi H, Hoshino K, Kaisho T, Sanjo H, Takeuchi O, Sugiyama M, Okabe M, Takeda K, Akira S. 2003. Role of adaptor TRIF in the MyD88-independent Toll-like receptor signaling pathway. *Science* 301:640–643. <http://dx.doi.org/10.1126/science.1087262>.
- Diebold SS, Kaisho T, Hemmi H, Akira S, Reis e Sousa C. 2004. Innate antiviral responses by means of TLR7-mediated recognition of single-stranded RNA. *Science* 303:1529–1531. <http://dx.doi.org/10.1126/science.1093616>.
- Latz E, Schoenemeyer A, Visintin A, Fitzgerald KA, Monks BG, Knetter CF, Lien E, Nilsen NJ, Espevik T, Golenbock DT. 2004. TLR9 signals after translocating from the ER to CpG DNA in the lysosome. *Nat Immunol* 5:190–198. <http://dx.doi.org/10.1038/ni1028>.
- Meurs EF, Breiman A. 2007. The interferon inducing pathways and the hepatitis C virus. *World J Gastroenterol* 13:2446–2454. <http://dx.doi.org/10.3748/wjg.v13.i17.2446>.
- Hornung V, Ellegast J, Kim S, Brzózka K, Jung A, Kato H, Poeck H, Akira S, Conzelmann KK, Schlee M, Endres S, Hartmann G. 2006. 5'-Triphosphate RNA is the ligand for RIG-I. *Science* 314:994–997. <http://dx.doi.org/10.1126/science.1132505>.
- Kato H, Takeuchi O, Sato S, Yoneyama M, Yamamoto M, Matsui K, Uematsu S, Jung A, Kawai T, Ishii KJ, Yamaguchi O, Otsu K, Tsujimura T, Koh CS, Reis e Sousa C, Matsuura Y, Fujita T, Akira S. 2006. Differential roles of MDA5 and RIG-I helicases in the recognition of RNA viruses. *Nature* 441:101–105. <http://dx.doi.org/10.1038/nature04734>.
- Hou F, Sun L, Zheng H, Skaug B, Jiang QX, Chen ZJ. 2011. MAVS forms functional prion-like aggregates to activate and propagate antiviral innate immune response. *Cell* 146:448–461. <http://dx.doi.org/10.1016/j.cell.2011.06.041>.
- Saha SK, Pietras EM, He JQ, Kang JR, Liu SY, Oganessian G, Shahangian A, Zarnegar B, Shiba TL, Wang Y, Cheng G. 2006. Regulation of antiviral responses by a direct and specific interaction between TRAF3 and Cardif. *EMBO J* 25:3257–3263. <http://dx.doi.org/10.1038/sj.emboj.7601220>.
- Zhong B, Yang Y, Li S, Wang YY, Li Y, Diao F, Lei C, He X, Zhang L, Tien P, Shu HB. 2008. The adaptor protein MITA links virus-sensing receptors to IRF3 transcription factor activation. *Immunity* 29:538–550. <http://dx.doi.org/10.1016/j.immuni.2008.09.003>.
- Stack J, Haga IR, Schröder M, Bartlett NW, Maloney G, Reading PC, Fitzgerald KA, Smith GL, Bowie AG. 2005. Vaccinia virus protein A46R targets multiple toll-like-interleukin-1 receptor adaptors and contributes to virulence. *J Exp Med* 201:1007–1018. <http://dx.doi.org/10.1084/jem.20041442>.
- Stack J, Bowie AG. 2012. Poxviral protein A46 antagonizes Toll-like receptor 4 signaling by targeting BB loop motifs in toll-IL-1 receptor adaptor proteins to disrupt receptor:adaptor interactions. *J Biol Chem* 287:22672–22682. <http://dx.doi.org/10.1074/jbc.M112.349225>.
- Lysakova-Devine T, Keogh B, Harrington B, Nagpal K, Halle A, Golenbock DT, Monie T, Bowie AG. 2010. Viral inhibitory peptide of TLR4, a peptide derived from vaccinia protein A46, specifically inhibits TLR4 by directly targeting MyD88 adaptor-like and TRIF-related adaptor mole-

- cule. *J Immunol* 185:4261–4271. <http://dx.doi.org/10.4049/jimmunol.1002013>.
16. Harte MT, Haga IR, Maloney G, Gray P, Reading PC, Bartlett NW, Smith GL, Bowie A, O'Neill LA. 2003. The poxvirus protein A52R targets Toll-like receptor signaling complexes to suppress host defense. *J Exp Med* 197:343–351. <http://dx.doi.org/10.1084/jem.20021652>.
  17. Bowie A, Kiss-Toth E, Symons JA, Smith GL, Dower SK, O'Neill LA. 2000. A46R and A52R from vaccinia virus are antagonists of host IL-1 and Toll-like receptor signaling. *Proc Natl Acad Sci U S A* 97:10162–10167. <http://dx.doi.org/10.1073/pnas.160027697>.
  18. DiPerna G, Stack J, Bowie AG, Boyd A, Kotwal G, Zhang Z, Arvikar S, Latz E, Fitzgerald KA, Marshall WL. 2004. Poxvirus protein N1L targets the I-kappaB kinase complex, inhibits signaling to NF-kappaB by the tumor necrosis factor superfamily of receptors, and inhibits NF-kappaB and IRF3 signaling by Toll-like receptors. *J Biol Chem* 279:36570–36578. <http://dx.doi.org/10.1074/jbc.M400567200>.
  19. Mibayashi M, Martínez-Sobrido L, Loo YM, Cárdenas WB, Gale M, Jr, García-Sastre A. 2007. Inhibition of retinoic acid-inducible gene I-mediated induction of beta interferon by the NS1 protein of influenza A virus. *J Virol* 81:514–524. <http://dx.doi.org/10.1128/JVI.01265-06>.
  20. Pachler K, Vlasak R. 2011. Influenza C virus NS1 protein counteracts RIG-I-mediated IFN signalling. *Virology* 418:48. <http://dx.doi.org/10.1016/j.virus.2011.08.008>.
  21. Andrejeva J, Childs KS, Young DF, Carlos TS, Stock N, Goodbourn S, Randall RE. 2004. The V proteins of paramyxoviruses bind the IFN-inducible RNA helicase, mda-5, and inhibit its activation of the IFN-beta promoter. *Proc Natl Acad Sci U S A* 101:17264–17269. <http://dx.doi.org/10.1073/pnas.0407639101>.
  22. Irie T, Kiyotani K, Igarashi T, Yoshida A, Sakaguchi T. 2012. Inhibition of interferon regulatory factor 3 activation by paramyxovirus V protein. *J Virol* 86:7136–7145. <http://dx.doi.org/10.1128/JVI.06705-11>.
  23. Rassa JC, Meyers JL, Zhang Y, Kudravalli R, Ross SR. 2002. Murine retroviruses activate B cells via interaction with Toll-like receptor 4. *Proc Natl Acad Sci U S A* 99:2281–2286. <http://dx.doi.org/10.1073/pnas.042355399>.
  24. Kurt-Jones EA, Popova L, Kwinn L, Haynes LM, Jones LP, Tripp RA, Walsh EE, Freeman MW, Golenbock DT, Anderson LJ, Finberg RW. 2000. Pattern recognition receptors TLR4 and CD14 mediate response to respiratory syncytial virus. *Nat Immunol* 1:398–401. <http://dx.doi.org/10.1038/80833>.
  25. Mogensen TH, Paludan SR. 2005. Reading the viral signature by Toll-like receptors and other pattern recognition receptors. *J Mol Med (Berl)* 83:180–192. <http://dx.doi.org/10.1007/s00109-004-0620-6>.
  26. Wang Y, Cao YL, Yang F, Zhang Y, Wang SH, Liu L. 2010. Small interfering RNA effectively inhibits the expression of SARS coronavirus membrane gene at two novel targeting sites. *Molecules* 15:7197–7207. <http://dx.doi.org/10.3390/molecules15107197>.
  27. O'Neill LA, Bowie AG. 2007. The family of five: TIR-domain-containing adaptors in Toll-like receptor signalling. *Nat Rev Immunol* 7:353–364. <http://dx.doi.org/10.1038/nri2079>.
  28. Xie P. 2013. TRAF molecules in cell signaling and in human diseases. *J Mol Signal* 8:7. <http://dx.doi.org/10.1186/1750-2187-8-7>.
  29. Häcker H, Tseng PH, Karin M. 2011. Expanding TRAF function: TRAF3 as a tri-faced immune regulator. *Nat Rev Immunol* 11:457–468. <http://dx.doi.org/10.1038/nri2998>.
  30. Palleroni AV, Varesio L, Wright RB, Brunda MJ. 1991. Tumoricidal alveolar macrophage and tumor infiltrating macrophage cell lines. *Int J Cancer* 49:296–302. <http://dx.doi.org/10.1002/ijc.2910490226>.
  31. Cleveland JL, Jansen HW, Bister K, Fredrickson TN, Morse HC, III, Ihle JN, Rapp UR. 1986. Interaction between Raf and Myc oncogenes in transformation in vivo and in vitro. *J Cell Biochem* 30:195–218. <http://dx.doi.org/10.1002/jcb.240300303>.
  32. Erridge C, Kennedy S, Spickett CM, Webb DJ. 2008. Oxidized phospholipid inhibition of Toll-like receptor (TLR) signaling is restricted to TLR2 and TLR4: roles for CD14, LPS-binding protein, and MD2 as targets for specificity of inhibition. *J Biol Chem* 283:24748–24759. <http://dx.doi.org/10.1074/jbc.M800352200>.
  33. Gay NJ, Symmons MF, Gangloff M, Bryant CE. 2014. Assembly and localization of Toll-like receptor signalling complexes. *Nat Rev Immunol* 14:546–558. <http://dx.doi.org/10.1038/nri3713>.
  34. Siu KL, Kok KH, Ng MH, Poon VK, Yuen KY, Zheng BJ, Jin DY. 2009. Severe acute respiratory syndrome coronavirus M protein inhibits type I interferon production by impeding the formation of TRAF3.TANK.TBK1/IKKepsilon complex. *J Biol Chem* 284:16202–16209. <http://dx.doi.org/10.1074/jbc.M109.008227>.
  35. Huang Y, Yang ZY, Kong WP, Nabel GJ. 2004. Generation of synthetic severe acute respiratory syndrome coronavirus pseudoparticles: implications for assembly and vaccine production. *J Virol* 78:12557–12565. <http://dx.doi.org/10.1128/JVI.78.22.12557-12565.2004>.
  36. Takeuchi O, Akira S. 2010. Pattern recognition receptors and inflammation. *Cell* 140:805–820. <http://dx.doi.org/10.1016/j.cell.2010.01.022>.
  37. Kumar H, Kawai T, Akira S. 2011. Pathogen recognition by the innate immune system. *Int Rev Immunol* 30:16–34. <http://dx.doi.org/10.3109/08830185.2010.529976>.
  38. TenOever BR, Servant MJ, Grandvaux N, Lin R, Hiscott J. 2002. Recognition of the measles virus nucleocapsid as a mechanism of IRF-3 activation. *J Virol* 76:3659–3669. <http://dx.doi.org/10.1128/JVI.76.8.3659-3669.2002>.
  39. TenOever BR, Sharma S, Zou W, Sun Q, Grandvaux N, Julkunen I, Hemmi H, Yamamoto M, Akira S, Yeh WC, Lin R, Hiscott J. 2004. Activation of TBK1 and IKKvarepsilon kinases by vesicular stomatitis virus infection and the role of viral ribonucleoprotein in the development of interferon antiviral immunity. *J Virol* 78:10636–10649. <http://dx.doi.org/10.1128/JVI.78.19.10636-10649.2004>.
  40. Tseng YT, Wang SM, Huang KJ, Lee AI, Chiang CC, Wang CT. 2010. Self-assembly of severe acute respiratory syndrome coronavirus membrane protein. *J Biol Chem* 285:12862–12872. <http://dx.doi.org/10.1074/jbc.M109.030270>.
  41. Chan CM, Ma CW, Chan WY, Chan HY. 2007. The SARS-coronavirus membrane protein induces apoptosis through modulating the Akt survival pathway. *Arch Biochem Biophys* 459:197–207. <http://dx.doi.org/10.1016/j.abb.2007.01.012>.
  42. Fang X, Gao J, Zheng H, Li B, Kong L, Zhang Y, Wang W, Zeng Y, Ye L. 2007. The membrane protein of SARS-CoV suppresses NF-kappaB activation. *J Med Virol* 79:1431–1439. <http://dx.doi.org/10.1002/jmv.20953>.
  43. Hu Y, Wen J, Tang L, Zhang H, Zhang X, Li Y, Wang J, Han Y, Li G, Shi J, Tian X, Jiang F, Zhao X, Liu S, Zeng C, Wang J, Yang H. 2003. The M protein of SARS-CoV: basic structural and immunological properties. *Genomics Proteomics Bioinformatics* 1:118–130.
  44. Pacciarini F, Ghezzi S, Canducci F, Sims A, Sampaolo M, Ferioli E, Clementi M, Poli G, Conaldi PG, Baric R, Vicenzi E. 2008. Persistent replication of severe acute respiratory syndrome coronavirus in human tubular kidney cells selects for adaptive mutations in the membrane protein. *J Virol* 82:5137–5144. <http://dx.doi.org/10.1128/JVI.00096-08>.
  45. Chen HZ, Wen Q, Wang WJ, He JP, Wu Q. 2013. The orphan nuclear receptor TR3/Nur77 regulates ER stress and induces apoptosis via interaction with TRAPγ. *Int J Biochem Cell Biol* 45:1600–1609. <http://dx.doi.org/10.1016/j.biocel.2013.04.026>.